ific
rine
Environmental
Laboratory

Annual Report for FY 89

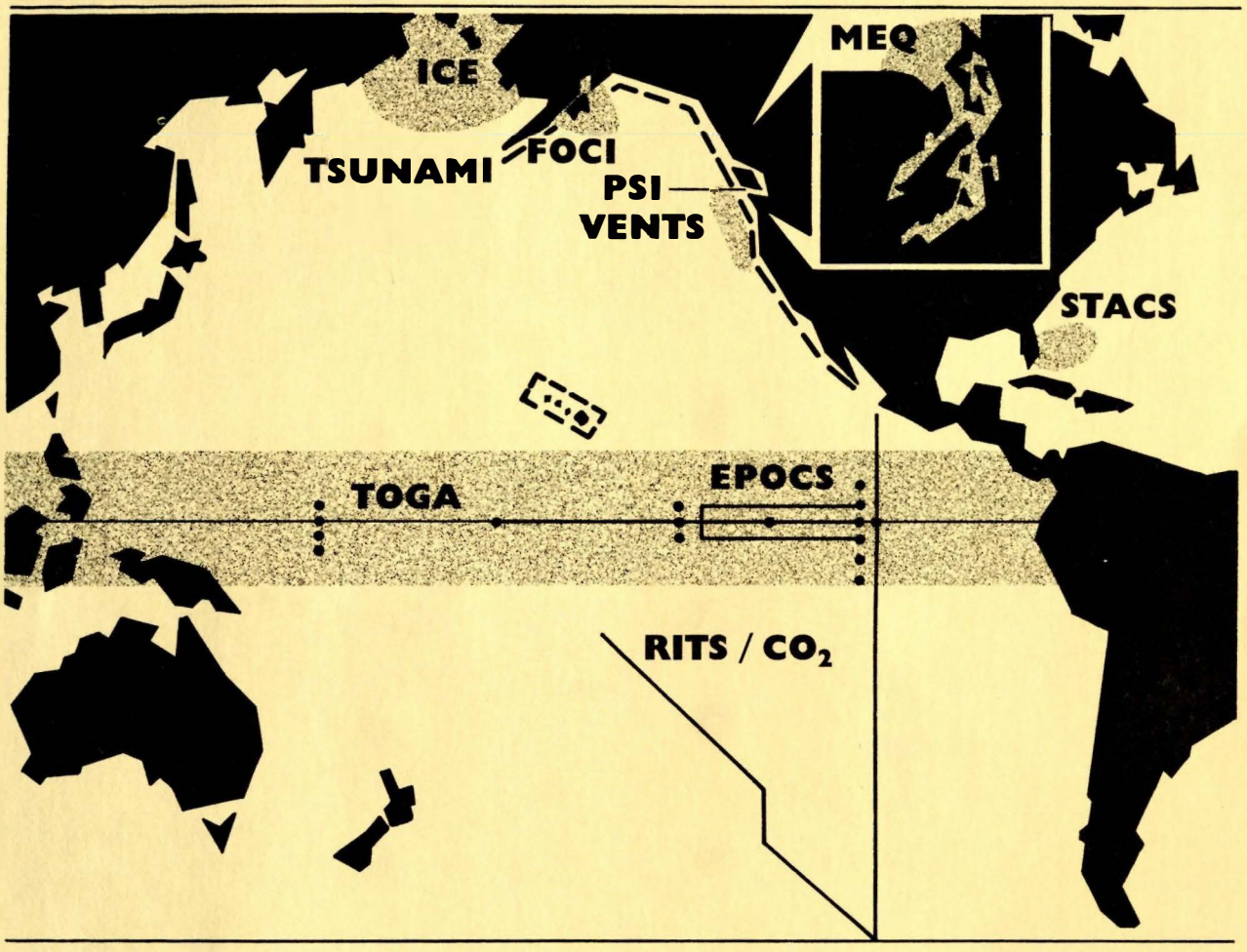

U.S. Department of Commerce
National Oceanic and Atmospheric Administration
Environmental Research Laboratories

PACIFIC MARINE ENVIRONMENTAL LABORATORY ANNUAL REPORT FISCAL YEAR 1989

January, 1990

Pacific Marine Environmental Laboratory
7600 Sand Point Way NE
Seattle, WA 98115

UNITED STATES DEPARTMENT OF COMMERCE

Robert A. Mosbacher
Secretary

NATIONAL OCEANIC AND ATMOSPHERIC ADMINISTRATION

John A. Knauss
Under Secretary for Oceans and Atmosphere/Administrator

Environmental Research Laboratories

Joseph O. Fletcher
Director

NOTICE

Mention of a commercial company or product does not constitute an endorsement by NOAA/ERL. Use of information from this publication concerning proprietary products or the tests of such products for publicity or advertising purposes is not authorized.

CONTENTS

Page

INTRODUCTION 1

CLIMATE RESEARCH 2

EQUATORIAL DYNAMICS 2
WESTERN BOUNDARY CURRENTS 4
MARINE AND ATMOSPHERIC CHEMISTRY FOR CLIMATE CHANGE 4

MARINE RESOURCES 7

VENTS PROGRAM 7
FISHERIES-OCEANOGRAPHY COORDINATED INVESTIGATIONS (FOCI) 10

MARINE OBSERVATION AND PREDICTION 14

ARCTIC RESEARCH 14
TSUNAMIS 16

MARINE ENVIRONMENTAL ASSESSMENT 18

LONG-RANGE-EFFECTS RESEARCH 18

JIMAR 21

JISAO 25

CIMRS 27

PMEL Staff 29

PMEL Seminars 33

JISAO Seminars 36

JIMAR Seminars 40

PMEL Publications 42

JISAO Publications 66

JIMAR Publications 67

CIMRS Publications 70

GLOSSARY OF ACRONYMS 71

INTRODUCTION

E.N. Bernard, Director

The Pacific Marine Environmental Laboratory (PMEL) conducts interdisciplinary scientific investigations in oceanography, marine meteorology, and related subjects. Current PMEL programs focus on climate, marine observation and prediction, marine resources, and marine environmental assessment. Studies are conducted to improve our understanding of the complex physical and geochemical processes that determine the extent of human effect on the marine environment; to define the forcing functions and the processes driving ocean circulation and the global climate system; and to improve environmental forecasting capabilities and other supporting services for marine commerce and fisheries.

PMEL complements its research efforts through three Environmental Research Laboratory (ERL) cooperative institutes: the Joint Institute for Study of the Atmosphere and Ocean (JISAO), with the University of Washington; the Joint Institute for Marine and Atmospheric Research (JIMAR), with the University of Hawaii; and the Cooperative Institute for Marine Resources Studies (CIMRS), with Oregon State University. PMEL also complements its research through the National Marine Fisheries Service (NMFS).

CLIMATE RESEARCH

The National Oceanic and Atmospheric Administration (NOAA) Ocean Climate Program was developed following the passage of the National Climate Program Act in 1978 in response to increased public awareness of the effects of short- and long-term climatic changes and a concern about the potential impact of technology and population growth on world climate.

Understanding and forecasting climatic change requires an understanding of the processes of heat, moisture, and momentum exchange between the ocean and atmosphere as well as the large-scale transports of heat within the atmosphere and ocean. PMEL's ocean climate research program conducts studies of both local and basin-wide ocean dynamics and the coupled ocean-atmosphere circulation, with the goal of determining the physical mechanisms that generate anomalies in sea-surface temperature (SST) distributions in the tropical ocean. A crucial step is to develop and validate ocean circulation models that are capable of simulating the evolution of globally important events such as El Niño.

Heat transport by major western boundary currents (the Gulf Stream and the Kuroshio in the Northern Hemisphere) is also postulated to have an important effect on world climate. Western boundary current studies at PMEL continue to focus on the Florida Current as part of the Sub-tropical Atlantic Climate Studies (STACS).

Accomplishments FY 89

EQUATORIAL DYNAMICS

In support of the Tropical Ocean and Global Atmosphere (TOGA) program, PMEL maintains an array of moored and island stations in the tropical Pacific. A total of 21 moored stations measure the vertical distribution of the current velocity, temperature, and salinity between the surface and 500 m on the equator and the temperature profile down to 500 m off the equator. Both types of moorings transmit wind velocity, air temperature, and SST in real time; in addition, the currents at 10 m and the off-equatorial temperature profiles are also reported in real time.

Automated wind stations are also maintained on islands in the western and central Pacific (Kapingamarangi, Nauru, Baker, and Christmas Island). The data from these stations are used collectively, along with other data sets, to diagnose the current state of the tropical Pacific, to validate the operational ocean general circulation model (GMC) at the National Meteorological Center (NMC), and to study air-sea interaction processes responsible for annual and interannual variability of the tropical Pacific.

Influence of SST on Surface Winds

The influence of SST on surface winds is at the heart of understanding the coupled ocean-atmosphere system. A recently completed study used the moored wind and SST measurements in the eastern tropical Pacific, where SST gradients are large and variable, to examine this problem.

The Equatorial Front lies at about 2°N. During the boreal fall cold season, SST across the front changes by several degrees in 200 km. The front is advected by the monthly surface current variability associated with the tropical instability waves. This signal, which is not directly forced by the local winds, provides an interesting probe for investigating the effects of SST changes on surface winds. Correlations of SST and surface-wind changes showed that the southeast tradewinds were enhanced when they crossed from the equatorial cold tongue to the warmer water north of the front. This effect suggests that boundary layer stratification is an important component of the surface-wind dynamics. Unstable stratification (cool air over warm water) allows the low level jet, a common feature of the eastern Pacific, to penetrate to the surface, yielding higher surface wind. This effect needs to be incorporated into the operational atmospheric models and the simple coupled El Niño-Southern Oscillation (ENSO) models if more realistic ocean-atmosphere feedbacks are to be obtained.

Role of extra-equatorial Rossby waves in El Niño events

A new compilation of historical bathythermograph (BT) data in the tropical Pacific allowed the observation of westward-propagating long Rossby waves in the northern tropical Pacific. The new BT data show that although the Rossby waves can be very important in determining pycnocline anomalies to the west of regions of strong wind-stress-curl forcing (both on annual and interannual periods), there is little evidence that the waves reflect off the western boundary to affect subsequent evolution of a warm event on the equator; e.g., a trigger for the onset of El Niño. Modeling studies which show that ENSO-like behavior can be generated with no involvement of extra-equatorial waves support the BT data.

Ocean modeling

Considerable progress was made this year using the Geophysical Fluid Dynamics Laboratory (GFDL) ocean circulation model to explore possible types of response in the central and eastern equatorial Pacific to multi-day-duration episodes of surface westerly winds in the equatorial western Pacific. The model shows that forcing from a 10-day wind event can lead to SST warming for as long as several months later in the far east and along the central American coast. Further observational and modeling work is needed to examine the importance of such forcing in real ENSO events.

WESTERN BOUNDARY CURRENTS

The Florida Current transport is continuing to be derived from observations of the cross-stream cable voltages between Jupiter, FL, and Settlement Point, Grand Bahama Island. The 7 years of data have been carefully scrutinized for errors, edited using improved estimates of the geomagnetic and tidal variations, and adjusted for the long-term decrease in the calibration factor caused by the secular change in the earth's magnetic field. The new magnetic station at Settlement Point now permits the removal of the geomagnetic variations on a daily to weekly basis. The voltage stability of the cable-seawater contact at West Palm Beach is also under study using an Ag-AgCl electrode installed in the ocean near the power station.

MARINE AND ATMOSPHERIC CHEMISTRY FOR CLIMATE CHANGE

PMEL conducts two important marine chemistry programs for NOAA under the National Climate Program. One program studies how the ocean affects the atmospheric concentration of several climatically important trace species. This study focuses on the biogeochemical cycles of carbon, sulfur, nitrogen and oxygen. The other program measures the changing concentration of anthropogenic fluorocarbons in the ocean to elucidate pathways and rates of thermocline ventilation and circulation.

Biogeochemical Cycles

PMEL conducted two field programs in 1989 to study the climate forcing trace gases and aerosols that affect climate. The first, a round trip cruise from Seattle south along 105°W to 61°S aboard the NOAA ship *Discoverer*, carried 25 scientists from 11 institutions. During the cruise scientists measured the carbon cycle trace gases (CO_2, CO, and CH_4) in surface waters by continuous, automated gas chromatography. Carbon dioxide and alkalinity concentrations were also measured at various depths in the water column. The major sulfur species in seawater (dimethylsulfide) and the atmosphere (dimethylsulfide, sulfur dioxide, sulfate, and methanesulfonate) were also measured to assess the ocean's role in the formation of sulfate aerosol particles.

The second major field project, called the Pacific Stratus Investigation (PSI), was a multi-agency (NOAA, National Aeronautics and Space Administration (NASA), National Science Foundation (NSF), Department of Energy (DOE), and Department of Defense (DOD)) interdisciplinary study of the effect of the sulfur cycle on marine stratus clouds and climate. The study, conducted off the Washington coast, included measurements from the NOAA ship *McArthur*, a coastal research station at Cheeka Peak, three research aircraft, and the Advanced Very-High-Resolution Radiometer (AVHRR) satellites.

PMEL also participated in NASA CITE-3 sulfur intercomparison studies designed to intercalibrate the various research groups around the world making sulfur measurements and to compare various measurement techniques.

Tracer Program

As part of the *Discoverer* cruise, a freon tracer survey collected more than 1700 samples to produce a unique image of the ventilation of the southeast Pacific thermocline, a region where no measurements of freon or any other transient tracers had ever been made. In addition to documenting the freon transient invasion into the Antarctic Intermediate Waters, PMEL scientists were able to detect a freon signal in the recently ventilated Antarctic Bottom Waters. These data, and similar measurements along 150°W/170°W in 1984, are the only existing freon values in the high southern latitudes of the Pacific. They are being used by the World Ocean Circulation Experiments (WOCE) tracer community to guide their ship-track and sampling plans for the pan-Pacific survey scheduled for 1990–93. The data are also being used in collaborative work with GFDL to validate global ocean circulation models.

Plans FY 90

EQUATORIAL DYNAMICS

- Complete data collection and begin analysis of moored measurements in the Pacific North Equatorial Countercurrent.
- Begin the diagnosis of SST and upper ocean heat content variability in the western equatorial Pacific warm pool using moored wind, current, temperature and salinity time series.
- Begin the analysis of equatorial current variations on a basin scale from a moored current meter array spanning 110°W–147°E in collaboration with U.S. and non-U.S. investigators.
- Develop a real-time capability for current profiles in the equatorial ocean.
- Expand TOGA TAO array in western Pacific with cooperation of Japan. This expansion will also be part of a pilot study for the TOGA Coupled Ocean-Atmosphere Response Experiment (COARE) in the warm pool regions of the western Pacific.
- Complete studies of the mechanisms of seasonal warming and cooling in the equatorial waveguide, using model and observational studies of the seasonal cycle.

WESTERN BOUNDARY CURRENTS

- Install a voltage-recording system for the Key West-Havana abandoned cable.
- Continue to study and improve the cross-stream measurements of Florida Current.
- Study suitability of various telephone cables for monitoring ocean transport.

MARINE AND ATMOSPHERIC CHEMISTRY FOR CLIMATE CHANGE

- Conduct a major international oceanographic/atmospheric expedition in the Pacific Ocean aboard the U.S.S.R. research vessel *Academic Korolev* to study the photochemistry and ocean-atmosphere exchange of the equatorial marine boundary layer and the freon distributions in the source waters of the North Pacific Intermediate Water near Kamchatka and into the Sea of Okhotsk.

- Conduct a second multi-agency study off the Washington Coast to study the effect of the marine sulfur cycle on stratus clouds and climate.

- Complete a study of the Deep Western Boundary Current in the southwest Pacific Ocean to improve our understanding of the invasion of freon tracers into the abyssal waters of the Pacific Ocean.

- Participate in both a freon intercalibration with WOCE and a sulfur intercalibration with NSF.

MARINE RESOURCES

Accomplishments FY 89

VENTS PROGRAM

Hydrothermal venting, now known to occur along the entire global seafloor spreading-center system, is a significant contributor to the heat and mass budgets of the ocean. In order to quantify, and eventually predict, the thermal and chemical oceanographic consequences of venting, the VENTS Program is engaged in a multidisciplinary effort to (1) determine the effects and fate of hydrothermal mass and heat on seawater through chemical and geochemical studies, (2) determine the physical oceanographic processes whereby hydrothermal heat, chemicals, and gases are distributed throughout the ocean, and (3) determine conditions that control the location, style, and duration of active venting through geological and geophysical studies.

VENTS laboratory and field programs involve collaboration with scientists from the United States Geological Survey, the Geological Survey of Canada, the Universities of Washington, Oregon State, Florida, Michigan, California (Scripps), Hawaii, and Victoria (Canada), Florida Institute of Technology, Moss Landing Marine Laboratories, Lamont-Doherty Geological Observatory and Woods Hole Oceanographic Institution.

During 1989, field investigations of the Juan de Fuca Ridge were concentrated in two regions, the southern Juan de Fuca Cleft Segment and the Cobb Segment which is the northernmost segment of the Juan de Fuca Ridge.

Two new chemical techniques were successfully attempted in the field during FY 89. In cooperation with scientists from Moss Landing Marine Laboratories, an in-situ chemical analysis system was coupled to a conductivity-temperature-depth (CTD) gauge to continuously map the distribution of iron and manganese in vent hydrothermal plumes. This is the first time that the distribution of chemical hydrothermal parameters has been mapped with the same degree of detail as hydrographic parameters, an advancement that will greatly enhance quantitative evaluation of chemical reactions in hydrothermal plumes. In cooperation with scientists from Florida Institute of Technology, large-volume samples of plume particles were collected by means of an in situ pump and filter unit. These samples will be particularly useful for studying the role of hydrothermal particles as scavengers of chemicals from seawater. Dissolved phosphate profiles normal to the ridge axis indicated large negative anomalies (up to 100 nmol L^{-1}) over vent fields which are attributable to scavenging processes. Mass-balance calculations suggest that hydrothermal scavenging accounts for 17%, 40%, and 40%, respectively, of the P, V, and As sinks in the ocean.

Physical oceanography studies have continued to focus on determining flow characteristics that transport hydrothermal plumes away from the Juan de Fuca Ridge. Data from year-long current-meter mooring deployments during 1987–88, on the saddle between Axial and Brown Bear Seamounts, revealed an oscillating flow with a frequency of about 4 days together with a long-term average flow of 4 cm s^{-1} to the south. These measurements suggest a possible alternating exchange of water north and south of the Cobb-Eickelberg seamount chain throughout the year. The water transported from north of the Cobb-Eickelberg chain is about 0.05°C warmer than the water south of the chain. Combined CTD and current-meter observations suggest southward flow along the entire east side of the Juan de Fuca Ridge. On the west side, the Axial-Brown Bear saddle may be near a convergence zone between southward and northward currents which then flow westward. The highly energetic environment on the saddle suggests that other gaps in the ridge and seamount chains may be important in determining the regional distribution of hydrothermal effluents.

Complementing the results just cited, analysis of data from a large-scale array of current-meter moorings from 1987–88 was initiated. Three additional moorings, deployed in 1988 to monitor the megaplume region and to measure flow variability west of the ridge along the south side of the Vance Seamounts, were recovered in 1989. Additional moorings were deployed in 1989 to further examine the effect of the Cobb-Eickelberg Seamount chain on large-scale water movements and to continue monitoring the megaplume area.

The processing of all northeast Pacific spreading-center Sea Beam data collected during the period from 1980 to 1988 was completed in FY 89 and the results assembled in a digital data base. Detailed bathymetric maps of any area of the northeast Pacific spreading-center plate boundary now can be produced at any scale. Advanced image-processing and digital signal-processing techniques have been developed for use with sidescan sonar data, resulting in greatly improved imagery of detailed seafloor morphology.

During FY 89, a pilot study was initiated to detect episodic seafloor events along the northeast Pacific spreading-center system by means of T-phases received on Pacific Missile Range/Missile Impact Location System hydrophone arrays. Other studies have demonstrated that acoustic energy from such events can be utilized to provide a much more sensitive threshold of detection than is feasible by means of conventional P and S phases sensed by land-based seismic arrays. Moreover, T-phases are also capable of providing information about the nature of an event's source. T-phases have been used to discriminate between submarine volcanic eruptions, shallow and deep earthquakes, and manmade explosions. Objectives of the study include (1) monitoring of earthquakes and/or volcanic activity along the northeast Pacific spreading-center system, (2) establishing relationships between ridgecrest earthquakes, volcanic activity, and hydrothermal venting, and (3) detecting active submarine eruptions.

Northern Juan de Fuca Ridge

The FY 89 VENTS Program continued its efforts to identify all major venting sites on the Juan de Fuca Ridge and to assess the effects of the emissions from those sites on the regional hydrography and chemistry of the northeast Pacific Ocean. In FY 89 a continuous CTD/

transmissometer tow-yo was made of the Endeavour Ridge and the Cobb Segment of the Juan de Fuca Ridge. The only major venting source encountered was the known field at 48°N on the Endeavour Ridge. Minor plumes were encountered over the topographic high of the Cobb Segment around 47°43′N. Hydrothermal emissions may also be occurring through sediments at the northern end of the Cobb Segment, but confirmation of venting there awaits further chemical analysis.

A large-scale grid of 35 stations extending from 20 km east to 140 km west of the Cobb Segment was also occupied during FY 89. This grid is analogous to a similar grid of stations around the southern Juan de Fuca Ridge occupied in FY 88. When data from these stations are fully analyzed they will form a unique data set for understanding the large-scale impact of hydrothermal venting on the hydrography and chemistry of the ocean waters adjacent to the Juan de Fuca Ridge.

Central Juan de Fuca Ridge

During FY 89, a PMEL-designed bottom pressure recorder (BPR) was deployed within the caldera of Axial Volcano. Analysis of the initial BPR data indicates that the summit area of the volcano is currently in a dynamic phase, evidenced by ground deformation caused by magma deflation, possible eruptions, or shallow magma intrusions on the southeast flank. Ideal-body modeling of subsurface structure based on seafloor gravity measurements indicates shallow low-density material underlies both the central caldera and southeast rift zone. Analysis of sea-surface gravity over Axial indicates the presence of a significant anomaly which appears to be the hotspot which created Axial Volcano and the rest of the Cobb-Eickelberg Seamount Chain. The gravity anomaly is located beneath the volcano's southern rift zone.

In FY 89, a special issue of a geophysical research journal was dedicated to a series of papers focused on the last few years of interdisciplinary research at Axial Volcano. NOAA VENTS Program investigators and their collaborators contributed a large number of manuscripts dealing with research topics including: (1) high-resolution bathymetry and geological mapping of the caldera and the vent site, (2) evidence of ground deformation and its possible relationship to active venting, (3) hydrography of the non-buoyant hydrothermal plume, (4) regional oceanographic circulation around Axial Volcano, (5) gravity surveys of Axial Volcano, (6) distribution and composition of particulates carried in the non-buoyant hydrothermal plume, (7) relationships between the distribution of hydrothermal fluids in the vent field and boiling hydrothermal fluids, and (8) the chemistry of phase-separated hydrothermal fluids.

Southern Juan de Fuca Ridge

Data collected annually since 1986 at the northern end of the Cleft Segment, where the megaplume event was discovered, indicated a consistent and continuing change in the chemistry of the vent fluids being emitted in this region. It is hypothesized that the megaplume was triggered by a tectonic disturbance of the northern Cleft Segment spreading center which resulted in a cataclysmic release of a very large volume of high-temperature vent fluid. Since the time of the

original megaplume discoveries, there has been a continuous reequilibration of the chemistry of vent fluids coming from this region. The VENTS Program has been tracking these changes to understand this unique example of non-steady-state venting behavior.

A major objective during FY 89 was to determine the geological setting of the Megaplume Site in order to test hypotheses for the formation of the megaplume and investigate the nature of the hydrothermal venting giving rise to the megaplume. The continuing presence of a vigorous "normal" hydrothermal plume (100–200 above the seafloor) mapped near the ridge crest between 44°53′N and 45°00′N suggests that the megaplume was generated along this portion of the ridgecrest. Initial mapping from the *Discoverer* using a deep-towed camera system revealed an extensive zone of semi-continuous venting over a distance of about 12 km. In the southern portion of the area, the venting is associated with fissuring of older volcanic terrain. In the northern part of the area, a very young lava flow was discovered. These preliminary observations suggest that this portion of the rift valley is undergoing tectonic extension accompanied by extrusive volcanism.

Eleven *Alvin* dives were conducted at the close of FY 88 in this area to sample the vent fluids as well as to geologically assess the area as the probable source region of observed megaplume events. All of the vents in this region were found to occur along a young fracture system marking the contact between the old and young volcanics. Virtually continuous venting (up to 60°C) was occurring over a distance of at least 4 km. In the northernmost part of the region, venting was occurring at approximately 100-m intervals along a 1-km-long fissure that was the source of recent volcanic flows. Extinct sulfide chimneys were found along lineaments within a few hundred meters east and west of this hydrothermally active fissure system.

FISHERIES OCEANOGRAPHY COORDINATED INVESTIGATIONS

Each year there are fluctuations in the quantity of commercially valuable fish and shellfish in the Gulf of Alaska and Bering Sea. To understand the causes of variability in recruitment to these stocks, scientists from PMEL and the Alaska Fisheries Science Center have been conducting Fisheries Oceanography Coordinated Investigations (FOCI). The present focus of the program is on walleye pollock (*Theragra Chalcogramma*) in the western Gulf of Alaska. Research has been directed at determining (1) what meteorological, oceanographic and biological conditions are correlated with historical year-class success, (2) whether interannual variations in transport affect larval concentrations, and (3) how mortality is affected by small-scale physics, food availability, and predation.

A vital step toward understanding the relation of pollock to the environment was undertaken this year. A numerical model was developed to examine the time-dependent dispersion of larvae. The model produces contours of larval concentrations on a 1-by-1-km grid which spans the entire study area. This approach allows a natural integration of biotic and abiotic data. Observations of the velocity field from satellite and in-situ platforms provide estimates of advection and diffusion. Estimates of hatching and mortality rates from sequential cruises provide source and sink terms. As development of the basic model continues, tests of soundness of the necessary approximations will be examined by simulating historical distribution patterns of larvae. In addi-

tion to intrinsic value, the model will be a useful tool in determining the direction of the field program.

During the 1989 field season, an experiment was conducted to examine the impact of over-water winds on vertical structure of the horizontal current field. Measurements were successfully made from an Atlas-type surface buoy using System ARGOS data transmission. Current measurements were collected using an acoustic Doppler current profiling instrument moored 65 m below the surface.

Observations from previous years suggests biotic and abiotic differences in environmental conditions between Alaska Coastal Current (ACC) and nearshore waters. These differences may have significant impact on survival of pollock larvae. For 1989, an experiment was designed to provide a description of transport and biological conditions in the two regions. Observations were collected from moored instruments, aboard ship and from satellite images (AVHRR). Measurements included acoustic Doppler current profiles, fluorescence, microzooplankton, towed net camera and conductivity and temperature versus depth. Preliminary analyses show strong differences in zooplankton concentrations across the Shelikof sea valley. When all data sets are processed, the analysis of these data will answer the question of different survival rates and provide valuable input to the model.

Plans FY 90

VENTS PROGRAM

- Continue monitoring plume intensity and distribution at the northern Cleft venting site.
- Continue long-term mooring deployments.
- Conduct a detailed sediment trap experiment at the northern Cleft Segment vent site.
- Conduct a large-scale hydrographic and chemical survey around Axial Volcano.
- Conduct an *Alvin* submersible program at the northern end of the Cleft Segment, i.e., the Megaplume Site, with geological and chemical objectives including resolution of the present discrepancy between water-column indications of active high-temperature venting and the fact that only low-temperature venting has been observed on the seafloor.
- Model the relationship between the heat, major element, and seawater content of the hydrothermal fluids within the buoyant plume regime located at the southern end of the Cleft Segment.
- Continue developing the capability to make in-situ measurements of the concentrations of dissolved Mn, Fe, and Si.

- Initiate the development of a capability to measure the concentration of dissolved Mn by flow injection analysis and chemiluminescence.

- Continue development of the VENTS Submersible-coupled in-situ Sensing and Sampling System (SIS^3) by enhancing capabilities of in-submersible control/data logging modules.

- Conduct geological and geophysical, chemical, and physical oceanographic surveys from the *Discoverer* at the megaplume sites and at Axial Volcano.

- Analyze the results of FY 89 surveys.

- Continue the analysis of the heat-^{3}He-Si relationships in off-axis regions.

- Continue the analysis of dissolved vs. particulate phase relationships for trace elements in the water column over active vent sites.

- Analyze sediment-trap materials for major and trace elements and determine chemical fluxes to the sediments in on- and off-axis regions west of the Juan de Fuca Ridge.

- Refine models of the rates and processes that control the physical and chemical evolution of vent fluids as they mix with ambient seawater and are dispersed away from the vent field.

- Analyze large-scale CTD observations collected during the past 4 years and integrate these results with water-column chemical data to document regional hydrothermal chemical anomalies.

- Synthesize all current-meter measurements.

- Plan and implement an interdisciplinary hydrothermal flux experiment on the southern Juan de Fuca Ridge.

- Develop (in collaboration with Scripps Institution of Oceanography investigators) a seafloor-deformation monitoring instrument and deploy it in the caldera of Axial Volcano in mid-1990.

- Develop and deploy two improved BPR instruments. These instruments, in conjunction with the seafloor deformation instrument, will provide unambiguous monitoring of seafloor vertical ground deformation and local seismicity.

- Analyze the data from a surface gravity and magnetics survey of the entire southern Juan de Fuca Ridge, to be completed during the 1989 field season.

- Monitor tectonic/volcanic processes in the megaplume area by, (1) deploying a short-term, ocean-bottom seismometer array, (2) making seafloor gravity measurements, and (3) conducting an active seismic-refraction survey.

- Continue to merge sidescan-sonar, water-column, and photogeological information into an integrated digital data base for compilation into detailed hydrothermal-parameter maps.

- Continue to refine the quantitative ability of reconnaissance sidescan-sonar survey data to discriminate specific seafloor geological (including hydrothermal) environments.

- Analyze existing T-phase data along the Gorda Ridge for evidence of tectonic and volcanic activity.

- Initiate efforts to reactivate the Midway Pacific Missile Range/Missile Impact Location System hydrophone array as well as other arrays in the Aleutian Islands and off California with the overall objective of establishing tectonic/volcanic/hydrothermal event detection along Pacific spreading centers.

FISHERIES OCEANOGRAPHY COORDINATED INVESTIGATIONS

- Obtain estimates of divergence of velocity which affects patches of pollock larvae using LORAN-C tracked buoys.

- Continue long-term monitoring of water properties, pollock egg and larval distributions; continue satellite image analysis to define the mean current on all spatial scales.

- Continue model development and use the model as a tool to help establish priorities of field and laboratory studies.

- Conduct preliminary analysis of physical data collected to examine difference between ACC and nearshore waters.

- Use long-term current, water property, and climatological data to establish a monthly mean description of the physical environment.

- Conduct an experiment to observe concurrent over-water and island winds together with horizontal current profiles.

- Examine integration FOCI data sets with larger data bases to investigate relationships on basin wide and climate scales.

MARINE OBSERVATION AND PREDICTION

Accomplishments FY 89

ARCTIC RESEARCH

The Beaufort Sea Mesoscale Circulation Study

The Outer Continental Shelf (OCS) Beaufort Sea study was completed. The principal conclusions of the study are:

- Below the upper 40–50 m, the major circulation feature of the outer shelf and slope is the Beaufort Undercurrent, a strong flow which in the mean is directed eastward but which is subject to frequent reversals toward the west. These reversals are normally accompanied by upwelling onto the outer shelf. The undercurrent is very likely part of a basin-scale circulation within the Arctic Ocean.

- While the influence of the wind on the subsurface flow in the southern Beaufort Sea is statistically significant, it is generally of secondary importance and accounts for less than 25% of the flow variance below 60 m. Therefore, below the mixed layer the circulation on the relatively narrow Beaufort shelf is primarily forced by the ocean rather than local winds.

- There are large changes in wind variance with season, with the largest variance occurring in late summer/early autumn and again in January because blocking ridges in the north Pacific shift the storm track westward over the west coast of Alaska and across the North Slope.

- Despite the seasonally varying wind field and the large seasonal differences in the upper-ocean temperature and salinity fields, there is no evidence for a seasonal variability in the subsurface circulation. This situation contrasts with that in Bering Strait, and probably also in much of the Chukchi Sea, where a seasonal wind-driven cycle in the transport is readily apparent.

- During 1986–87, the Beaufort Undercurrent appears to have been anomalously deep by 30–40 m. The consequences of such anomalies for the upper-ocean velocity structure and transport are likely significant.

- Both 1986 and 1987 were warmer than normal, with less coastal ice in the summer and autumn and more storms passing along the west coast of Alaska and across the North Slope. These climatological near-minimum ice years were followed in 1988 by the heaviest summer ice along the Chukchi coast since 1975.

- The atmospheric sea-level pressure field was well represented by the Fleet Numerical Oceanography Center (FNOC) surface analysis if the 12-hour lag of the FNOC pressures is taken into account. However, the FNOC surface air temperature field shows a systematic over-prediction during winter and spring of 10–20°C, leading to an annual over-prediction of air temperature by 3–13°C.

The FREEZE Experiment

The FREEZE experiment, begun in 1987, continued the study of finescale and mesoscale processes related to ice formation over the western arctic shelves. A combination of current meter and pressure gauge moorings were used to estimate dynamical effects, drifting ice buoys to trace ice motion and ice edge advance, and CTD surveys to map heat and salt budgets prior to and during initial fall freezeup.

Investigations in the Greenland Sea

Convection and water-mass transformation in the Greenland Sea, which is being studied under the International Greenland Sea Project (IGSP), is of major consequence to the ventilation of the deep ocean. During FY 89 PMEL was involved in five of the IGSP cruises and an instrument deployment to monitor the Denmark Strait overflow. The work employs long-term moored instrument arrays and seasonally repeated hydrographic censuses of very high accuracy. Preliminary examination of the hydrographic data suggests that during 1988–89 the upper 2 kilometers of the ocean were successfully ventilated following several years of little, if any, deep convection.

Two new instrumented arrays were deployed in 1989 to monitor the southwestern part of the Greenland Sea, where recirculation from the East Greenland Current may provide fresh water to the convective gyre. The gyre appears to be rather delicately poised with respect to its ability to sustain convection so that small variations in the fresh water supply can alter or stop the convection.

Sea Ice Processes and Modeling

As a major step in improving forecasts of coastal sea ice motion around Alaska, the existing one-dimensional (1-D) coastal sea ice/barotropic ocean model is being expanded to two dimensions conforming to the topography of the western arctic shelves. The new model has nominal 18-km grid spacing, employs the ice thickness/strength relation developed for the 1-D model, and retains both the barotropic and wind-driven forcing critical to ice motion on these shelves. The effects of different lateral boundary conditions are being examined together with a sensitivity study of the various model parameters. The model is expected to lead to a full forecasting capability for the Navy/NOAA Joint Ice Center in 2 to 3 years.

Coordinated Eastern Arctic Experiment (CEAREX)

The objective of the PMEL CEAREX effort is to collect a comprehensive high-Arctic meteorological data set covering fall through spring. The regional pressure gradient was determined from drifting buoys, while radiation, atmospheric soundings, and near-surface wind and temperature profiles were measured from a drifting ship and ice camp. During spring, two flights were made over the ice camp with the NOAA P3 research aircraft, providing detailed observations of the vertical variation of turbulence, wind, and temperature. A regional atmospheric model will be developed capable of improving ice forecasting and climate models by including the low level temperature inversion structure found in the Arctic in winter.

Vessel Icing

At high latitudes, spray generated by ships in heavy seas can freeze to vessel structures, producing an extreme hazard. The operational NOAA vessel icing forecast algorithm was evaluated against advances in understanding the icing process and against recent operational experience. The NOAA algorithm shows excellent results when compared with a new cold-water data set from the Labrador Sea, as well as having provided excellent forecasts to over 140 fishing vessels in Alaskan waters during late January 1989, the worst icing episode of the decade.

TSUNAMIS

The long-term goal of the Tsunami Project is to improve our understanding of the dynamics of tsunami generation, propagation, and shoreline inundation. To this end, the PACific Tsunami Observation Program (PACTOP) was developed to acquire high-quality tsunami measurements in the deep ocean and coastal environment. Continuous maintenance of the PACTOP deep ocean network required three cruises in 1989 to recover and re-deploy bottom pressure recorders (BPRs) and collect CTD data.

Existing BPRs were modified to collect data at 15-second intervals, compared to the old data rate of about 1 minute. This will greatly improve our measurements of small, higher frequency, tsunamis. The increased data rate will also allow the study of seismic surface waves which may play an important role in the physics of tsunami generation. In this regard, a collaborative effort was initiated with scientists at the Scripps Institute of Oceanography who developed a differential pressure gauge for the study of microseisms. The instrument was deployed in the Shumagin Seismic Gap, a seismically active region characterized by significant tsunamigenic earthquake potential.

Data reduction, analysis, and numerical modeling efforts focused on three small tsunamis generated in the Gulf of Alaska on 17 and 30 November 1987 and 6 March 1988. These events were recorded by PACTOP BPRs and by coastal tide gauges. These data were used to test a surface deformation model to compute estimates of the vertical seafloor displacement. Several tsunami simulations were performed, and a preliminary comparison with the BPR observations indicates

good agreement in the case of the 6 March tsunami, but poor agreement for that of 30 November. These preliminary results demonstrate the critical nature of accurate tsunami source specification. The results also suggest that the simple earthquake fault plane model for the 6 March event is perhaps more realistic than that for 30 November, possibly due to inaccuracies in the seismologically derived fault plane parameters for 30 November, or to a fundamental inadequacy of the rectangular fault plane idealization to deal with more complex earthquake mechanisms.

Plans FY 90

ARCTIC RESEARCH

- Continue analysis of the circulation on the Alaskan shelves, including effects of upwelling and Pacific inflow.
- Develop a cooperative shelf circulation research program with the U.S.S.R., focusing on the Chukchi Sea.
- Recover the FREEZE moorings from the northern Bering and Chukchi seas, and complete a third survey of the western arctic shelves during autumn 1989.
- Calibrate and process the 1988–89 IGSP data set, and analyze earlier moored measurements in the recirculation region of the southern Greenland Sea.
- Recover moored arrays in the Greenland Sea during June-July 1990.
- Apply the 2-D sea ice/barotropic ocean model to the Bering and Chukchi seas, and perform a sensitivity study of the model with historical climate data.
- Compare CEAREX ice/atmosphere data with an atmospheric model for the Arctic.

TSUNAMIS

- Complete comparison of numerical tsunami simulations and deep-ocean measurements.
- Maintain the PACTOP network by the recovery and redeployment of all deep-ocean BPRs.

MARINE ENVIRONMENTAL ASSESSMENT

Accomplishments FY 89

LONG-RANGE-EFFECTS RESEARCH

Marine environmental assessment at PMEL emphasizes understanding of the complex physical and geochemical processes that ultimately determine the health of marine systems and their ability to assimilate contaminants. Included are studies of the geochemistry of trace metals and organic compounds, distributions of hydrocarbons and synthetic organics, coastal and estuarine circulation, and transport processes. Although the geographic focus of these studies has been Pacific Northwest and Alaskan coastal and estuarine waters, the scientific knowledge acquired and methodologies developed are applicable to other marine systems.

Estuarine Circulation

During 1989, the study of bottom-water intrusions focused on temporal variations in the onset of intrusions as a result of fluctuations in the horizontal density gradient caused by salinity variations across the sill in the Strait of Juan de Fuca. Salinity changes outside the sill in the Strait of Juan de Fuca estuary appear to be the result of autumn and winter storms on the Pacific coast causing reversals of surface flow and variations in deep flow more than 135 km from the coast. These observations are the first to show that this effect can penetrate the full length of the Strait causing near-bottom salinity variations of sufficient magnitude to influence flow into Puget Sound. Although Puget Sound has characteristics of a fjord, calculations suggest that similar processes may occur in lower layer flow at the mouth of coastal plain estuaries.

A study of wind effects on non-tidal circulation in fjords was begun using observations from two prior experiments in Puget Sound. In contrast to other studies, which showed wind effects confined to the upper layer or compensating flow in a relatively thin layer beneath the pycnocline, compensating flows have occurred at middepths in Puget Sound with primarily outestuary winds and weaker stratification. Empirical orthogonal function (EOF) analysis of flow through two sections revealed two extremely different mean flow conditions, one with two-layer flow and one with approximately unidirectional flow. In addition, correlations between currents and winds in both cases are significant and negative with the flow from about 90–150 m in 200 m depth with about a 12-hour lag.

Contaminant Transport

The quantification of point and non-point inputs and an understanding of the physical and geochemical processes acting on contaminants are needed to understand the impact that humans are having on our nation's coastal regions. Using estuarine theory based on constituent-salinity correlations, a method to estimate non-point industrial inputs added to estuaries was developed. During wet weather, 60% of the dissolved Cu and Zn transported out of Elliott Bay, Washington, was found to have originated from non-point sources associated with shipyard activities. Wet-weather periods also produce high river flow which causes the formation of a thin surface layer of freshwater (<2 m) in Elliott Bay. Because of the short residence time of freshwater in the Bay (<1 day), dissolved metal contaminants added to the surface water are not adsorbed onto particles and few particles settle out of the freshwater surface lens. Since most of the transport of dissolved and particulate trace metals occurs during the wet season, little of the annual load of these trace metals are lost to the sediments of Elliott Bay.

Transport Modeling

A hydrodynamical model of Admiralty Inlet and the main basin of Puget Sound was completed and simulations of circulation and salinity are being compared with field measurements. The long, deep, and narrow character of Puget Sound allows for a laterally averaged, 2-D formulation. The reduced dimensionality permits simulations resolving tidal flows over time intervals of several months. The model differs from previous estuarine models in that it combines three elements essential to flow in Puget Sound: branched channel hydrodynamics, time-varying turbulence closure, and numerical techniques that prevent the artificial (numerical) diffusion of density fronts as they propagate into the estuary.

Some important results of the work are: (1) fortnightly variations of salinity in the Strait of Juan de Fuca dominate the control of quasi-fortnightly intrusions of dense water into the main basin of Puget Sound; (2) fresh water discharge from riverine sources is effectively trapped in the main basin by the vigorous vertical mixing in Admiralty Inlet; (3) vertical advection speeds approaching 1 cm s^{-1} are possible at some locations in the Sound; (4) evanescent internal tides appear in the main basin after periods of sufficient fresh water discharge; and (5) downward mixing of fresher Whidbey basin discharge occurs during southerly winds and at time of intrusions. This circulation model permits the creation of a time series of advection and mixing fields requisite for subsequent models of particulate and chemical tracer transport.

The vertical transport of a chemical tracer in Puget Sound has been explored with a two-stage scavenging model. In the first stage, a dissolved tracer is scavenged by and desorbed from fine particulates while at the same time the fine particulates are scavenged and settled by macroaggregates. Application of the model to ^{234}Th data from Puget Sound sets the time scale for fine particle scavenging near 6 days, while disaggregation of the macroaggregates occur at time scales of only a few days. These processes control the speed at which contaminants are removed from the water column to the bottom sediments.

Work on the Puget Sound Reflux Model was completed. Results indicate that for the main basin only about one-third of the upper layer's seaward flow refluxes landward within Admiralty Inlet. This is one-half of previous estimates which were incomplete due to the neglect of side channels and the lack of adequate salinity and current data. Current work is now focused on the circulation physics of the region of maximum recirculation where about one-half of the surface seaward flow refluxes around Vashon Island. Calculations also show that the tracer lifespan within the estuary varies between 10 and 130 days depending upon the site of injection.

Sea Level in Puget Sound

A study of sea level in the Puget Sound region shows that most of the sea level fluctuations observed at Seattle propagate from the coastal region. For periods longer than 10 days, the amplitudes at Seattle are about 80% of those observed at Neah Bay, located 220 km away at the entrance to the Strait of Juan de Fuca. The winter fluctuations at Seattle lag those at Neah Bay with a time delay consistent with the propagation of barotropic waves. Highly variable from year to year, they are strongest during winter when storms impinge on the Washington and Oregon coasts. Groups of storms with low atmospheric pressure and southerly winds and separated by periods of high pressure and northerly winds produce a broad sea-level spectrum. Summer sea level is dominated by fortnightly fluctuations which vary greatly from year to year, unlike pure gravitational tides.

Plans FY 90

LONG-RANGE-EFFECTS RESEARCH

- Characterize the nature of Cu-organic interactions in Puget Sound during the FY 90 field season.
- Continue the study of sea-level processes in the Pacific Northwest.
- Continue the development of chemical dynamics models for estuaries.
- Understand and predict the mean seaward flow in Colvos Passage and the resulting recirculation around Vashon Island.
- Explore time-dependent scavenging models of tracer transport to evaluate water column residence times of chemical species.
- Examine the effects of wind on the circulation of Puget Sound using the laterally averaged model and a 1-D time-dependent model.

JIMAR

The Joint Institute for Marine and Atmospheric Research (JIMAR), located at the University of Hawaii, was formed in 1977, under a Memorandum of Understanding between the National Oceanic and Atmospheric Administration (NOAA) and the University of Hawaii. The principal research interests of JIMAR have been equatorial oceanography, climate, and tsunamis. A new interest in fisheries oceanography was added in FY 88.

Accomplishments FY 89

CLIMATE RESEARCH

JIMAR continued to produce, and publish in the Climate Analysis Center Bulletin, monthly subjectively analyzed mean surface wind fields for the Pacific. Diagnostic case studies of westerly wind bursts and their relation to El Niño-Southern Oscillation (ENSO) were also carried out.

A simple atmospheric model on an equatorial beta plane was used to study the coupling of a moist Kelvin wave with a low mode Rossby wave. An unstable mode which depends on the moisture convergence in the boundary layer has been described. The characteristics of the unstable mode are quite sensitive to the underlying sea-surface temperature (SST) distribution which determines the background state in the model.

Observational studies of the structure and propagation of Tropical Intraseasonal Waves were conducted. The data included outgoing longwave radiation plus 200 mb and 850 mb winds. Three major paths of propagation and the geographic dependence of the development were documented.

EQUATORIAL OCEANOGRAPHY

Analysis of the Pacific Equatorial Ocean Dynamics (PEQUOD) PEGASUS current profile data revealed the existence of three deep equatorial currents in the central Pacific below a depth of 1500 meters depth. Two of these have transports (7 Sverdrups; 1 Sverdrup = 10^6 m^3 s^{-1}) comparable to deep western boundary currents.

Analysis of the Western Equatorial Pacific Ocean Climate Studies (WEPOCS) data from the Celebes Sea revealed the structure of a number of currents, including the New Guinea Coastal undercurrent and the Mindanao current. Low-frequency variability in the area is a combination of local response to local winds and a large scale response to the monsoon.

The Hawaiian Ocean Time-series (HOT) project, a 5-year program of monthly biogeochemical and physical oceanographic observations at a station north of Oahu, conducted its first cruise in October 1988. Hydrographic observations and acoustic Doppler current profiles collected on the cruise are being analyzed.

A major workshop and planning meeting for the Coupled Ocean-Atmosphere Response Experiment (COARE) was held in Noumea in May 1989. Continued participation in this experiment is anticipated.

The Indo-Pacific sea-level network for Tropical Ocean and Global Atmosphere (TOGA) continued with four new stations in the Indian Ocean and two more Pacific stations upgraded to satellite transmission.

The TOGA Sea Level Center archived data for 72 of the 81 existing TOGA Pacific stations. There are 23 TOGA stations in the Indian Ocean, but data return is spotty.

A proposal was submitted to establish a sea-level center for the World Ocean Circulation Experiment (WOCE). This center would produce satellite transmitted data sets for distribution within a few months of the original data acquisition.

JIMAR scientists are included in the National Aeronautics and Space Administration's (NASA's) Topographic Experiment (TOPEX) Science Working Team.

FISHERIES OCEANOGRAPHY

The final two of five cruises to Southeast Hancock Seamount were completed in the fall of 1988. The biological and physical data are being analyzed. The description of the current patterns over the seamount is nearly complete. The acoustic Doppler current profiler data indicates that the flow at levels above the top of the seamount is nearly uniform in space over the seamount, but quite variable in time from one cruise to the next. The distribution of two micronekton species are being analyzed in relation to these current patterns.

A description of larval distribution relative to current patterns around Johnston Island was completed. The data indicate high abundances of island-related fish larvae downstream of the island. Analysis of larval distributions around Oahu continues. A field program to study the relationship of the distribution of larval lobster to oceanographic conditions in the Northwestern Hawaiian Islands is also underway.

TSUNAMI RESEARCH

Numerical studies to support the Pacific Tsunami Observational Program continued. A variety of different source distributions were used to generate tsunamis in two models with different depth and grid resolutions. The effects of varying the source parameters, as well as the effect of grid resolution, were investigated. Comparisons of numerical results with open ocean pressure

observations made during November 1987 and March 1988 were made. The numerical results are very sensitive to the assumed source parameters and the grid resolution.

An analysis of the tsunami evacuation zones for the state of Hawaii was begun, resulting in the redrawing of evacuation maps due to changing population patterns and urban development. The volunteer tsunami observer program has also been maintained, as has the publication of the Tsunami Journal.

Plans FY 90

CLIMATE RESEARCH

- Modeling studies of tropical low frequency motions including effects of non-linear heating and monsoonal basic flows.
- Tropical cyclone motion will be studied using a beta plane model with background mean flow.
- Comprehensive Ocean-Atmosphere Data Sets (COADS), outgoing longwave radiation (OLR), and sea level data will be used to study equatorial air-sea interaction on a variety of time scales, from several months to interannual.
- Continue to produce monthly surface wind maps for the Pacific.
- Develop calibration methods for satellite-based rainfall algorithms.
- Evaluate moored buoy wind data being taken for TOGA and Equatorial Pacific Ocean Climate Studies (EPOCS).
- Continue diagnostics studies of westerly wind events and low-frequency wind variability in the equatorial Pacific.

EQUATORIAL OCEANOGRAPHY

- Analysis and modeling of equatorial deep jets and El Niño current variability.
- Acoustic Doppler current profiler (ADCP) measurements will continue in TOGA and be proposed for WOCE.
- Continue to operate the Indo-Pacific sea level network.
- Continue to operate the TOGA Sea Level Center.

- Continue TOPEX work and prepare for acquisition of an operational sea-level data set supporting the TOPEX/POSEIDON altimeter data set.
- Continue the HOT project.
- Continue analysis of Line Islands Array and WEPOCS data.
- Continue COARE preparations, including publication of proceedings from the Noumea meeting, and preparation of an implementation plan.

FISHERIES OCEANOGRAPHY

- Analysis of the response of micronekton and other "oceanic" species to flow patterns around the summit of Southeast Hancock Seamount.
- Begin planning for a followup cruise to Johnston Island in FY 91.
- Physical and biological measurements will be made in the North Pacific Transition Zone to assess the impact of the large-mesh fishery on the pelagic fishes.

TSUNAMI RESEARCH

- Numerical studies of the sensitivity of tsunami models to the source parameters and grid resolution will continue to determine how model results can be sensibly compared with open ocean observations.
- Continue studying the problem of comparing near shore tide gauge records with open ocean pressure observations and numerical models.
- Complete the revised tsunami evacuation maps for the State of Hawaii.

JISAO

The Joint Institute for Study of the Atmosphere and Ocean (JISAO) was established to foster collaboration between the National Oceanic and Atmospheric Administration (NOAA) and the University of Washington. JISAO serves as a vehicle for funding grants and postdoctoral Fellows, and supporting collaborative research between NOAA and University scientists. During the past few years, JISAO has emphasized three core research areas: climate, environmental chemistry, and estuaries.

JISAO's climate research has tended to focus on two main themes: large-scale atmosphere-ocean interaction in the tropics and planetary-scale wave and mean flow interaction. These efforts have served to promote collaboration between PMEL and University scientists involved in theoretical and modeling studies of EPOCS. It has also been active in efforts to direct interdisciplinary research toward an understanding of the global climate system and its sensitivity to human activities. The new Environmental Climate Forecast Center within JISAO was established for this purpose.

The main research themes in environmental chemistry include marine aspects of the carbon dioxide problem, organic carbon dynamics, and chemical processes involving the deposition of heavy metals. Recently, JISAO's chemistry research has broadened in scope to include other biogeochemical cycles of interest for global climate. Of particular interest is the chemistry of sulfur and its influence on cloud condensation nuclei and the cycles that involve long-lived radiatively interactive trace species such as nitrous oxide and methane.

Accomplishments FY 89

JISAO scientists, in collaboration with NOAA scientists, were involved in a variety of climate research activities. In the field of modeling, scientists explored the sensitivity of interannual variability in a coupled ocean-atmosphere model to the physics parameterizations and climatological mean conditions, giving particular attention to identifying the stability of the coupled tropical ocean-atmosphere system. They also worked on the potential effect of cloud radiation feedback (CRF) on the El Niño-Southern Oscillation (ENSO) phenomenon and formulated a consistent yet simple model for the tropical atmosphere surface winds. Additionally, research was conducted in conjunction with the OCEAN STORMS field experiment, resulting in the analysis of a comma cloud-type storm using Nested-Grid Model (NGM) output and research aircraft observations.

Research concerning the propagation of equatorial waves also continued. In particular, researchers investigated the propagation of these waves in the presence of mean currents, studied the propagation of equatorial Kelvin waves on a sloping thermocline, investigated how a coastal

Kelvin wave can propagate on a sphere, and completed a study on aspects of Kelvin wave response to episodic wind forcing. Analysis aimed at clarifying the various mechanisms of oscillation in coupled ocean-atmosphere models also continued along with experiments using simple delayed-oscillator models to clear up points relating to the impact of stochastic forcing on the periodicity of such systems.

Work also continued in the area of environmental chemistry with the analysis of data collected on the RITS-88 [Radiatively Important Trace Species] cruise and a Pacific Stratus Experiment (PSI) cruise conducted in June off the Washington coast. Aerosol size distribution measurements, concentration, and chemical composition data from these cruises is under analysis.

Estuarine studies continue with research focusing on wind effects on non-tidal circulation in fjords. In addition to near-surface wind effects, mid-depth compensating flows have been documented in two separate experiments under different mean flow characteristics using both empirical orthogonal function (EOF) and lagged linear correlation analysis.

JISAO is also involved in research conducted at the Experimental Climate Forecast Center which began operation in January 1989. A computer system was acquired and work began on two problems: (1) exploring the predictability of the ENSO phenomenon and (2) examining the factors that influence climate change on time scales of 100 years.

Plans FY 90

- Work with NOAA to develop an expanding program for dealing with scientific issues relating to global climate change.
- Continue research on the predictability of ENSO events.
- Continue research on climate, focusing on coupled atmosphere-ocean interaction and biogeochemical cycles.
- Continue participation in research efforts involving Equatorial Pacific Ocean Climate Studies (EPOCS), Climate and Global Change, and PSI.
- Continue a vigorous visitor and seminar program.

CIMRS

The Cooperative Institute for Marine Resources Studies (CIMRS) was established in 1982 to foster collaborative research between NOAA and Oregon State University in the areas of oceanography, fisheries, aquaculture and other marine-related fields and to serve as a center at which researchers may addresss problems of mutual interest relating to the living and non-living components of the marine and estuarine environment and their interrelationships. Oregon State University is currently involved in research efforts that parallel NOAA/PMEL's VENTS Program objectives in the area of assessing the effect of spreading-center hydrothermal vents on the marine environment. CIMRS frequently funds grants which support collaborative research efforts between NOAA and University scientists. This annual report addresses only the collaborative efforts between CIMRS and NOAA/PMEL's VENTS Program.

Six CIMRS research assistants contribute directly to the VENTS Program in various components of computer support and scientific research on the Juan de Fuca Ridge. Significant accomplishments in computing capabilities include the development of software for sidescan sonar image enhancement, Sea Beam acoustic backscatter analysis and positioning of deeply towed vehicles with and without acoustic transponder navigation. Research programs centered on defining the tectonic and volcanological processes producing oceanic crust at the Juan de Fuca Ridge. Specific studies included the interpretation of geologic structure via seafloor remote-sensing techniques, determining seafloor physical properties from acoustic backscatter data, and the understanding of plate boundary mechanics from seismological investigations. Most significantly in FY 90 will be the addition of a postdoctoral fellow who is a specialist in numerical modelling of ridge-crest processes. It is anticipated that such models will provide a unifying framework for integrating various geophysical data sets which have been collected on the Juan de Fuca Ridge.

Accomplishments FY 89

- Published a paper on the geological structure of Axial Volcano, Juan de Fuca Ridge.
- Developed two new programs to assist in processing and analyzing ALVIN CTD data and is adapting a program to provide camera navigation for camera tows outside of transponder arrays.
- Prepared a paper on high resolution mapping of Axial Volcano, Juan de Fuca Ridge.
- Prepared a paper on enhanced imagery from side-scan sonar data using a very complex deconvolution technique.

- Prepared a paper on the relation of structure to earthquake size distribution on the Blanco Transform.

- Completed 85% of a composite database of SeaBeam bathymetric data over a five year period. This data was presented in a poster session at the 28th International Geological Congress for a session on "Morphology of Ocean Crust Formation." The completed data set will map 95% of the Juan de Fuca Ridge.

- Participated in the 1989 VENTS research cruise on the NOAA Ship DISCOVERER.

Plans FY 90

- Continue analysis and manipulation of SeaBeam backscatter data to determine the physical characteristics of the seafloor using the echo strength of the acoustic beam.

- Complete SeaBeam bathymetric database of Juan de Fuca Ridge, compile into user-friendly format for chart generation, create digital data base, and user's guide.

- Continue analysis of photogeologic data of seafloor from camera tows during FY 89 field season.

- Integrate gravity and magnetic surveys and SeaBeam data from the Juan de Fuca Ridge into models of crustal evolution.

PMEL STAFF

OFFICE OF THE DIRECTOR

Eddie N. Bernard, Director
James R. Holbrook, Deputy Director
LCDR Terry D. Jackson, Associate Director

Bernard, Eddie N.	Director
Cassady, Jeanne	Secretary (Typing)
Holbrook, James R.	Supervisory Oceanographer
Jackson, Terry D., LCDR	NOAA Corps
Wilson, Belle	Secretary (Typing)

TECHNICAL AND ADMINISTRATIVE SUPPORT

Cynthia L. Loitsch, Program Support Officer

Anderson, James W.	Photographer
Collins, Beverly J.	Budget Assistant
Cooke, Florence K.	Travel Clerk
Curl, Virginia M.	Illustrator
Elkins, Gayle L.	Motor Vehicle Operator
Loitsch, Cynthia L.	Program Support Manager
McLean, Allison	Computer Assistant
Perry, Richard M.	Motor Vehicle Operator
Smith, Claudia J.	Photographer
Snyder, Susan	Program Support Assistant
Thomasson, Norma H.	Support Services Supervisor
Taylor, Stashia*	Clerk-Typist
Vose, Virginia	Computer Clerk
Whitney, Ryan L.	Computer Operator

COMPUTER SUPPORT

Paul Lu, Computer Manager

Angkico, Susana L.	Computer Programmer
Barzel, Ronald	Communications Specialist
Bathurst, William	Computer Programmer
Beard, Emily, LTJG	NOAA Corps
Borg-Breen, David	Computer Systems Programmer
Kay, Sharon*	Computer Aid
Lu, Paul	Computer Specialist
McCarty, Laura C.	Computer Programmer
McGlothlen, Kenneth	Computer Assistant
Renton, Mark	JISAO/Research Scientist

* No longer affiliated with PMEL

Richards, Russel	Computer Equipment Analyst
Tanigawa, Dale	Computer Operator
Vance, Tiffany C.	Computer Programmer
Walker, Andrew D.	Computer Operator

ENGINEERING DEVELOPMENT DIVISION

Hugh B. Milburn, Division Leader

Delizo, Stan W.	Engineering Technician
Gable, James R.	Electronics Technician
Holzer, Dennis E.	Instrument Maker
Jackson, Thomas G.	Electronics Technician
Kinsey, Kevin	Laborer Technician
Mader, Floyd W.	Electronics Technician
McLain, Patrick D.	Electronics Engineer
Milburn, Hugh B.	Supervisory General Engineer
Miller, Hendrick	Engineering Technician
Nakamura, Alex I.	Electronics Engineer
Newman, Roy	Electronics Technician
Schattgen, Paul L., LTJG	NOAA Corps
Shanley, John C.	Engineering Aid
Stapp, Michael F.	Electronics Technician

MARINE ASSESSMENT RESEARCH DIVISION

Herbert C. Curl, Jr., Division Leader

Cannon, Glenn A.	Oceanographer
Cokelet, Edward D.	Oceanographer
Cudaback, Cynthia, LTJG	NOAA Corps
Curl, Herbert C., Jr.	Supervisory Oceanographer
Froberg, Sharon L.*	Physical Science Technician
Herzog, Carolyn	Secretary
Lavelle, John W.	Oceanographer
Lytle, Lisa*	Physical Science Aid
Mofjeld, Harold O.	Oceanographer
Murphy, Paulette P.	Chemist
Pashinski, David J.	Oceanographer
Paulson, Anthony J.	Oceanographer

MARINE RESOURCES RESEARCH DIVISION

Stephen R. Hammond, Division Leader

Appelgate, Bruce	CIMRS/Research Assistant
Baker, Edward T.	Oceanographer
Chadwick, William	CIMRS/Research Assistant
Clapp, Dan	CIMRS/Research Assistant
Dziak, Robert	CIMRS/Research Assistant
Eastham, Robin*	CIMRS/Clerk Typist

* No longer affiliated with PMEL

Embley, Robert W.	Geophysicist
Feely, Richard A.	Oceanographer
Fox, Christopher	Physical Scientist
Geiselman, Terri L.	Oceanographer
Gendron, James F.	Chemist
Hammond, Stephen R.	Supervisory Oceanographer
Hanneman, Susan*	CIMRS/Research Assistant
Jones, Frederick J., CDR	NOAA Corps
Lau, Andy	CIMRS/Research Assistant
Lebon, Geoffrey	JISAO/Research Scientist
Lemon, Michael, LTJG	NOAA Corps
Massoth, Gary J.	Oceanographer
Matsuura, Hiroshi	JISAO/Research Assistant
Murphy, Kim*	CIMRS/Research Assistant
Nitchman, Catherine, LTJG	NOAA Corps
Restrepo, Maria	CIMRS/Research Assistant
Roberts, Marilyn F.	Physical Science Technician
Rodarmel, Kimberly*	Secretary
Roe, Kevin K.	JISAO/Research Scientist
Salem, Brian*	Oceanographer
Seem, Dennis, LT	NOAA Corps
Tennant, David A.	Oceanographer
Waddell, Jessica	CIMRS/Administrative Assistant
Walker, Sharon L.	Oceanographer
Zervas, Chris	CIMRS/Research Assistant

MARINE SERVICES RESEARCH DIVISION

James E. Overland, Division Leader

Aagaard, Knut	Oceanographer
Berggren, Todd, LTJG	NOAA Corps
Blake, Wade J., LTJG	NOAA Corps
Bond, Nicholas	JISAO/Postdoctorate
Darnall, Clark	JISAO/Research Engineer
DeWitt, Carol	Physical Science Technician
Eble, Marie	Oceanographer
Gonzalez, Frank I.	Oceanographer
Gray, Judith G.	Meteorologist
Kachel, David G.	Computer Programmer
Lackmann, Gary M.*	JISAO/Research Assistant
Long, Virginia L.	Physical Science Technician
Macklin, Stewart A.	Meteorologist
Mattens, David M., LTJG*	NOAA Corps
Overland, James E.	Supervisory Oceanographer
Parker, William J.	Field Operations Specialist
Pease, Carol H.	Oceanographer
Proctor, Peter D.	Physical Science Aid
Reed, Ronald K.	Oceanographer
Roach, Andrew	Oceanographer
Salo, Sigrid	Oceanographer

* No longer affiliated with PMEL

Saucier, Suzanne*	Clerk-Typist
Schall, Marie	Physical Science Technician
Schumacher, James D.	Oceanographer
Stabeno, Phyllis	Oceanographer
Turet, Philip	JISAO/Research Scientist
Walter, Bernard A.*	Physical Scientist

OCEAN CLIMATE RESEARCH DIVISION

Stanley P. Hayes, Division Leader

Bates, Timothy S.	Research Chemist
Benson, Jeffrey	Physical Science Technician
Calhoun, Julie	JISAO/Graduate Research Assistant
Chang, Ping	JISAO/Postdoctorate
Coho, Carolyn S., ENS	NOAA Corps
Cole, Richard D.*	Physical Science Technician
Davison, Jerry C.	JISAO/Research Scientist
Freitag, Howard P.	Oceanographer
Gammon, Richard*	Supervisory Chemist
Giese, Benjamin S.*	JISAO/Research Assistant
Gifford, Sue E.	Secretary (Typing)
Hankin, Steven	Computer Programmer
Harrison, Don E.	Oceanographer
Hayes, Stanley P.	Supervisory Oceanographer
Johnson, Eric	NRC Postdoctorate
Johnson, James E.	JISAO/Research Scientist
Kelly, Kimberly C.	Oceanographer
Kessler, William S.*	JISAO/Research Assistant
LaConte, John	Electronics Technician
Larsen, Jimmy C.	Oceanographer
Lee, Daniel	JISAO/Scientific Programmer
Mangum, Linda J.	Oceanographer
Manke, Ansley B.	Computer Programmer
McCarty, Marguerite	JISAO/Scientific Programmer
McClurg, Dai	Computer Programmer
McPhaden, Michael	Oceanographer
McTaggart, Kristine	JISAO/Physical Science Technician
Meenen, Marilyn*	Clerk-Typist
Menzia, Fred	JISAO/Research Scientist
Moore, Ben A.	Electronics Technician
Pullen, Patricia E.	Oceanographer
Quinn, Patricia	CIRES/Postdoctorate
Shepherd, Andrew J.	Electronics Technician
Soreide, Nancy N.	Computer Programmer
Stratton, Linda	JISAO/Scientific Programmer
Taft, Bruce A.	Oceanographer
Verschell, Mark A.	JISAO/Scientific Programmer
Wilson, Clifford C., LTJG	NOAA Corps
Wisegarver, David P.	Chemist
Wolfe, Gordon	JISAO/Graduate Research Assistant

* No longer affiliated with PMEL

PMEL SEMINARS

Dates	*Name and Affiliation*	*Seminar Topic*
1988		
14 October	Dr. Hideo Kawai Kyoto University Japan	Divergence and entrainment in a river effluent: The heart-break model
22 November	Drs. Steve Clifford and Tom George NOAA's Wave Propagation Laboratory	Ocean remote sensing research at WPL/NOAA
12 December	Dr. Bernard Bonsang Centre des Faibles Radioactivites France	The marine source of light non-methane hydrocarbons: Application to the study of gas transfer between the ocean surface and the atmospheric boundary layer
15 December	Dr. Magne Haakstad Hogskole Senteret i Nordland Norway	Surface circulation in Hardanger Fjord
1989		
19 January	Dr. Phil Durkee Naval Post Graduate School Monterey, CA	Evidence for the effect of small aerosol particles on cloud reflectivity as observed from satellite data
26 January	Dr. Tony Hansen Lawrence Livermore Laboratory Livermore, CA	Aerosol black carbon measurements in remote locations
22 February	Dr. Chris Garrett Dalhousie University Nova Scotia Canada	Is the Mediterranean overmixed?
28 February	Dr. Jim Murray University of Washington Seattle, WA	New production in the eastern equatorial Pacific

6 March	Dr. Richard Reynolds NOAA Climate Analysis Center Camp Springs, MD	Surface momentum and heat fluxes from the NMC operational model
14 March	Dr. Curt Ebbesmeyer Evans-Hamilton Inc. USA	Teleconnection at low frequency (decadal period) between the North Pacific Ocean and Puget Sound's current structure
22 March	Dr. Eileen Hoffman Dept. of Oceanography Texas A & M University College Station, TX	Examples of physical/biological modeling studies
23 March	Dr. Peter Santschi Dept. of Marine Sciences Texas A & M University Galveston, TX	Trace metal scavenging in natural waters
30 March	Dr. Ken Johnson Moss Landing Marine Laboratory University of California at Santa Cruz Moss Landing, CA	Biogeochemistry of deep sea hydrothermal vent systems
20 April	Dr. Kelvin J. Richards Dept. of Oceanography Southhampton University	Fronts and layers in the equatorial Pacific Ocean
4 May	Dr. Victoria Fabry Woods Hole Oceanographic Institution Woods Hole, MA	Aragonite production in the open ocean: Shell growth rates of pteropod and heteropod molluscs
9 May	Dr. Mac Coon & Dr. Paula Lau BDM Corporation Seattle, WA	Ridge building and its implications for sea ice mechanics
11 May	Dr. Ann Gargett Institute of Ocean Sciences Sidney, B.C., Canada	Panama Basin water and thermohaline circulation
23 May	Mr. Dave Archer School of Oceanography University of Washington Seattle, WA	Calcite dissolution in deep sea sediments: An *in-situ* microelectrode study

20 June	Dr. Steve Emerson School of Oceanography University of Washington Seattle, WA	Molecular oxygen and delta 18-O in surface waters of the subarctic Pacific: Tracers of biological processes
10 July	Dr. Keith Dixon Geophysical Fluid Dynamics Laboratory	Simulation of chlorofluorocarbon transient tracer distribution in numerical models of the world ocean
21 August	Dr. John Bullister Woods Hole Oceanographic Institution Woods Hole, MA	Chloroflourocarbon studies in regions of deep water formation in the Atlantic

JISAO SEMINARS

Dates	*Name and Affiliation*	*Seminar Topic*
1988		
5 October	Dr. Dennis Moore JIMAR Honolulu, HI	The Coriolis force: (1) Introduction; (2) Inertial oscillations on Maclaurin's ellipsoid
27 October	Dr. Michael L. Banner School of Mathematics University of New South Wales Australia	Wave number spectra of short gravity waves
9 November	Dr. Richard Jahnke Skidaway Institute of Oceanography Savannah, GA	Organic matter cycling in Santa Monica Basin, California: The view from the bottom
10 November	"	Benthic fluxes: influence on ocean chemistry and an indicator of particle flux patterns
22 November	Dr. Tetsuo Nakazawa Goddard Space Flight Center Greenbelt, MD	Super cloud cluster over the western Pacific from GMS data
28 November	Dr. Sergei Kitaigorodskii Dept. of Earth and Planetary Sciences Johns Hopkins University Laurel, MD	The parameterization of surface fluxes and waves
29 November	"	Influence of background stable stratification on the parameters of geophysical turbulent boundary layers

1989

11 January	Dr. Catherine Goyet Woods Hole Oceanographic Institution Woods Hole, MA	Problems in the determination of the parameters of the CO_2 system in natural waters
13 January	"	Fiber optic sensor for direct measurement of the partial pressure of CO_2 in seawater: Principles and applications
13 January	Dr. Robert Charlson University of Washington Seattle, WA	Oceanic phytoplankton, atmospheric sulfur, cloud physics and climate
20 January	Dr. David Randall Colorado State University Fort Collins, CO	Interactions among radiation convection and large-scale dynamics in a GMC
14 February	Dr. Wallace S. Broecker Lamont-Doherty Geological Observatory Columbia University Palisades, NY	Do orbital cycles drive glaciation? If so, how?
15 February	"	The operation of the ocean during peak glacial time
	"	Predicting the climate of the 21st century: Lessons from the past
16 February	"	What caused the glacial to interglacial atmospheric CO_2 change?
17 February	Dr. Robert J. Delmas Grenoble, France	Long term climatic and environmental changes inferred from the vostok core
7 March	Dr. Hans Oeschger Universität Bern Bern, Switzerland	Rapid changes in climate and carbon dioxide: Evidence from polar ice cores (Cosponsored by Quaternary Research Center)
8 March	"	The carbon cycle and its natural and anthropogenic disturbances

28 March	Dr. Claus Hammer Geophysical Institute University of Copenhagen Denmark	Recent developments in ice core research with respect to past and present environments
29 March	"	Drastic climatic changes as observed in ice cores: What caused them? Will the greenhouse effect trigger a new ice age?
18 April	Dr. Jin-Song Max Planck Institüt für Meteorologie Hamburg, West Germany	The performance of four spectral GCMs on the southern hemisphere: The January and July climatology and the semiannual wave
18 April	Dr. Hans von Storch Max Planck Institüt für Meteorologie Hamburg, West Germany	ENSO-related numerical experiments with A-GCM, O-GCM and A/0-GCM at at the Max Planck Institüt
19 April	"	Principal oscillation pattern (POP) analysis: Concept, examples and generalization to principal interaction (PIP) analysis
20 April	Dr. Jin-Song Max Planck Institüt für Meteorologie Hamburg, West Germany	Prediction of the state of the SO using principal oscillation pattern analysis
5 May	Dr. Noboru Nakamura JISAO University of Washington Seattle, WA	Atmospheric heat budgets of the polar regions
12 May	Dr. Harry Hendon University of Colorado Boulder, CO	Australian summer monsoon dynamics
31 May	Dr. Sean A. Twomey University of Arizona Tuscon, AZ	Clouds, radiation and pollution
12 June	Dr. Eric Kraus Pagosa Springs, CO (formerly of CIRES)	Meridional heat transport in the ocean as calculated from internal oceanic data

13 June	Dr. Tom Malone St. Joseph College West Hartford, CN	Climate change, global change and science policy
14 June	Dr. Peggy Lemone NCAR Boulder, CO	Momentum transports in mesoscale convective systems
15 June	Dr. Brian Farrell Harvard University Cambridge, MA	Predictability of atmospheric flow
16 June	"	Transient developments in confluence and diffluence
30 June	Dr. Lee Panetta Texas A&M College Station, TX	Zonal jets in baroclinically active quasi-geostrophic turbulence: Phenomenology in simple models and speculations on observational analogs

JIMAR SEMINARS

Dates	*Name and Affiliation*	*Seminar Topic*
1988		
4 October	Brian King Institute of Oceanographic Sciences Wormley, England	Upper ocean studies in WEPOC's area
21 November	Dr. Valery K. Kedrinskii Lavrentyev Institute of Hydrodynamics, Novosibirsk, USSR Dr. Victor A. Akulichev Pacific Oceanological Institute, Vladivostok, USSR	Bubble dynamics in water and sea water inhomogeneities by acoustic methods
30 November	Dr. Kensuko Takeuchi Dept. of Geophysics Hokkaido University Hokkaido, Japan	The role of equatorial waves in El Niño/ Southern Oscillation events
1989		
14 March	Dr. Jix Song Xu Max Plank Institute Hamburg, West Germany	Prediction of the state of the southern oscillation using principal oscillation pattern analysis
11 May	Dr. George Adomian Applied Mathematics University of Athens Athens, GA	Solution of nonlinear systems (or how solve problems you thought impossible)
2 June	Dr. Lance Leslie Bureau of Meteorology Research Center Melbourne, Australia	Interactions of multiple vortices, with implications for tropical cyclones

JIMAR SEMINARS

Dates	*Name and Affiliation*	*Seminar Topic*
1988		
4 October	Brian King Institute of Oceanographic Sciences Wormley, England	Upper ocean studies in WEPOC's area
21 November	Dr. Valery K. Kedrinskii Lavrentyev Institute of Hydrodynamics, Novosibirsk, USSR Dr. Victor A. Akulichev Pacific Oceanological Institute, Vladivostok, USSR	Bubble dynamics in water and sea water inhomogeneities by acoustic methods
30 November	Dr. Kensuko Takeuchi Dept. of Geophysics Hokkaido University Hokkaido, Japan	The role of equatorial waves in El Niño/ Southern Oscillation events
1989		
14 March	Dr. Jix Song Xu Max Plank Institute Hamburg, West Germany	Prediction of the state of the southern oscillation using principal oscillation pattern analysis
11 May	Dr. George Adomian Applied Mathematics University of Athens Athens, GA	Solution of nonlinear systems (or how solve problems you thought impossible)
2 June	Dr. Lance Leslie Bureau of Meteorology Research Center Melbourne, Australia	Interactions of multiple vortices, with implications for tropical cyclones

29 June	Dr. David Karoly Centre for Dynamical Meteorology Monash University Melbourne, Australia	Southern hemisphere circulation features associated with El Niño-Southern Oscillation events
30 June	Dr. P.C. Sinha Centre for Atmospheric Sciences Indian Institute for Technology Delhi, India	Numerical simulation of coastal upwelling and vertical thermal structure in response to pure wind stress forcing in the western Bay of Bengal
27 July	Dr. Gregory Ruggerone College of Fisheries University of Washington Seattle, WA	Predator-prey interactions and fisheries management
18 August	Dr. Greg Holland Bureau of Meteorology Research Center Melbourne, Australia	Tropical cyclone motion
23 August	Dr. Julian P. McCreary Ocean Sciences Center Nova University Dania, FL	Numerical investigation of eastern boundary currents

PMEL PUBLICATIONS

AAGAARD, K. A synthesis of the Arctic Ocean circulation. *Rapports et Procès-verbaux des Réunions, Conseil international pour l'Exploration de la Mer* 188:11–22 (1989).

Moored current measurements in four different areas of the Arctic Ocean suggest that the principal large-scale advection occurs in narrow boundary currents along the margins of the major basins. These boundary flows are in a cyclonic sense in each basin and are therefore counter to much of the upper ocean drift suggested by the ice motion. In the interior of the Arctic Ocean (or at least in its Canadian Basin) the kinetic energy appears concentrated in the mesoscale eddy field, and there is evidence that this field is primarily generated along the Arctic Ocean margins. In addition, the Arctic Ocean has recently been found to sustain a large-scale thermohaline circulation driven by freezing along its periphery; this circulation appears to be at least comparable in magnitude to that of the Greenland Sea. If one also considers the major peripheral exchanges through the Fram Strait, the Barents Sea, the Canadian Archipelago, and the Bering Strait, then the image which emerges is of an Arctic Ocean which overwhelmingly is forced at its lateral boundaries, and in which much of the organized transport is trapped along these boundaries.

AAGAARD, K. Circulation: Beaufort Sea update. Proceedings, Alaska OCS Region 1987 Arctic Information Transfer Meeting Conference, OCS Study MMS 88–0040, Minerals Management Service, Anchorage, AK, 151–156 (1988).

No abstract.

BAKER, E.T., J.W. LAVELLE, R.A. FEELY, G.J. MASSOTH, S.L. WALKER, and J.E. Lupton. Episodic venting of hydrothermal fluids from the Juan de Fuca Ridge. *Journal of Geophysical Research* 94(B7):9237–9250 (1989).

Evidence of large-scale episodic venting of hydrothermal fluids was initially discovered in August 1986 in the form of a 130-km^3 radially symmetric "megaplume" over the southern Juan de Fuca Ridge. We report here on the discovery in September 1987 of a second, smaller megaplume about 45 km north of the location of the first megaplume. The ^{3}He/heat, ^{3}He/dissolved Mn, and ^{3}He/dissolved silica ratios in both megaplumes were typical of high-temperature vent fluids. Evidence from long-term records of current flow over the southern Juan de Fuca Ridge, and from the mineralogy and Mn chemistry of megaplume particles, makes it unlikely that the second megaplume was a reencounter of the first. A plume model that relates the heat flux to the observed plume rise height of ~1000 m finds that the total heat content of the fluids that formed the megaplumes was 10^{16}–10^{17} J, or

equivalently a fluid volume of 3–8 × 10^7 m^3 at 350°C. The geometry and suspended particle population of the first megaplume imply that such features are formed within a few days time. The extraordinary heat and volume fluxes associated with megaplumes (10^2–10^3 greater than ordinary vent fields), as well as their typical hydrothermal chemistry, suggest that they resulted from tectonic or hydraulic fracturing that suddenly increased the permeability of the hydrothermal fluid reservoir in the axial crust. The flux of hydrothermal heat from continuous venting and episodic megaplumes on the southern Juan de Fuca Ridge is presently 4–10 × 10^9 W, a factor of 5–10 greater than various geophysical model calculations for this ridge segment. This imbalance may be symptomatic of a recent surge in the local cycle of magmatic activity.

BATES, T.S. Evidence for the climatic role of marine biogenic sulfur. Ph.D. dissertation, University of Washington, Seattle, 99 pp. (1989).

The surface ocean plays an important role in the global biogeochemical sulfur cycle. Gaseous sulfur compounds emitted from the ocean are thought to be a major source of sulfate aerosol in the marine troposphere. Establishing the relationship between gaseous sulfur emissions, atmospheric sulfate concentrations, and aerosol particle populations is not only important in defining the ocean/atmosphere flux of sulfur, but also for the effects these particles may have on local cloud reflectivity, aerosol optical depth, and global climate. During 1982–1985, dimethylsulfide (DMS) concentrations were measured in over 1000 Pacific Ocean surface seawater samples. The data have been tabulated to take into account both regional and seasonal variations in concentration. These concentration data, combined with area-weighted summer and winter exchange coefficients, yield a net ocean to atmosphere DMS flux in the North Pacific Ocean of 0.12 ± 0.06 Tmol/a. Extrapolating this calculation by regional areas to the global ocean yields a net DMS flux of 0.50 ± 0.25 Tmol/a, less than earlier estimates of 1.2 Tmol/a, but still consistent with estimates of non-sea-salt sulfate deposition and model studies of the marine atmospheric sulfur budget. Using these regional and seasonal DMS concentration data, it appears that oceanic DMS emissions are positively correlated with atmospheric aerosol particle populations. The major components of the atmospheric biogeochemical sulfur cycle were measured along the coast of Washington State during May of 1987. Combining simultaneous measurements of the key oceanic and atmospheric sulfur species, it is possible to show the importance of DMS emissions on the cycling of sulfur in the marine boundary layer. Simultaneous measurements of oceanic DMS, atmospheric aerosol sulfate and the size-resolved physical properties of the aerosol were made in the equatorial Pacific during July 1987. Under light and variable winds, in an area free of continental and anthropogenic air masses, an observed increase in oceanic DMS concentrations preceded simultaneous increases in non-sea salt sulfate aerosol, the fraction of volatile sub-micrometer (sub-μm) aerosol, the aerosol particle population, and the mean particle diameter of the sub-μm aerosol. These data support the hypothesis that oceanic DMS is the source of background marine sulfate aerosols formed from gas-to-particle conversions in the atmosphere.

Betzer, P.R., K.L. Carder, R.A. Duce, J.T. Merrill, N.W. Tindale, M. Uematsu, D.K. Costello, R.W. Young, R.A. FEELY, J.A. Breland, R.E. Bernstein, and A.M. Greco. A pulse of asian dust to the central north pacific: long-range transport of giant mineral aerosol particles. *Nature* 336(6199):568–571 (1988).

Several recent studies have shown that large quantities of mineral dust from eastern Asia are transported through the atmosphere to the North Pacific each spring. The paucity of information on mineral fluxes during individual dust events prompted a coordinated effort, Asian Dust Input to the Oceanic System (ADIOS), which simultaneously measured mineral fluxes in the atmosphere and upper water column during such an event. In March 1986 a major dust outbreak in China moved over the North Pacific Ocean and was detected downstream using changes in particle number, size and composition. Most striking was the presence of "giant" (>75–μm) silica minerals found in atmospheric as well as water-column samples at the ADIOS sampling site (26°N, 155°W). Their appearance more than 10,000 km from their source cannot be explained using currently acknowledged atmospheric transport mechanisms. Furthermore, the large wind-blown minerals that dominated our samples are extremely rare in the long-term sedimentary record in the North Pacific.

Calhoun, J.A., and T.S. BATES. Sulfur isotope ratios: tracers of non-sea salt sulfate in the remote atmosphere. In *Biogenic Sulfur in the Environment*, E.S. Saltzman and W.J. Cooper (eds.), American Chemical Society Symposium Series No. 393, 367–379 (1989).

The atmospheric biogeochemical sulfur cycle is being significantly impacted by increasing anthropogenic sulfur emissions. The effect of these emissions on the concentration of sulfate aerosol particles in the remote marine atmosphere is difficult to assess due to uncertainties surrounding the relative contributions of natural and anthropogenic sources. Sulfur isotope ratios can be used to determine the relative magnitude of these sources in the remote atmosphere provided 1) the isotopic ratios of the potential sulfur sources are known, 2) the isotopic compositions of the various sources are different from one another, and 3) the isotopic changes that occur during transformations are thoroughly documented. In the text which follows, these aspects of sulfur isotope chemistry are addressed. Isotopic interpretation of sulfur sources to the remote atmosphere is severely limited by the absence of critical isotopic measurements, yet it appears that continental sulfur sources are isotopically distinguishable from seasalt or marine biogenic sulfur sources. Improved analytical techniques will soon provide the means to obtain the necessary data.

CANNON, G.A. Time variations of bottom-water inflow at the mouth of an estuary. In *Understanding the Estuary: Advances in Chesapeake Bay Research*, Proceedings of a Conference, March 28–31, 1988, Baltimore, MD, Chesapeake Research Consortium Publication 129, CBP/TRS 24/88, 424–427 (1988).

Puget Sound is a fjord-like estuary, but its 30-km long entrance sill, Admiralty Inlet, has characteristics very similar to coastal plain estuaries. The replacement of bottom water in Puget Sound has been studied for many years, because it is a dominant process responsible

for flushing some contaminants. Previous studies showed bottom-water inflow increased during neap tides when mixing was minimal over the entrance sill. Recent observations show the increased inflow starts before minimum neap tides, and simple model calculations with these data demonstrate this is an effect of variations in the horizontal density gradient at the mouth of the estuary caused by salinity variations outside the mouth. This time-dependent process may be responsible for changing inflow characteristics at time scales between wind effects and seasonal effects, and it may be important in other estuaries such as Chesapeake Bay.

Charlson, R.J., and T.S. BATES. The role of the sulfur cycle in cloud microphysics, cloud albedo, and climate. Preprints, Symposium on the Role of Clouds in Atmospheric Chemistry and Global Climate, Jan. 30-Feb. 2, 1989, Anaheim, CA, American Meteorological Society, Boston, MA, 1–3 (1989).

No abstract.

Chen, C.T.A., R.A. FEELY, and J.F. GENDRON. Lysocline, calcium carbonate compensation depth, and calcareous sediments in the North Pacific Ocean. *Pacific Science* 42(3–4):237–252 (1988).

An extensive oceanographic investigation has been carried out in the North Pacific Ocean. The purpose of this report is to present the results of two cruises in which we participated and to report additional carbonate data from samples collected for us in the North Pacific. These data are combined with data from the literature to provide an overall picture of the carbonate system in the North Pacific. The degree of saturation of seawater with respect to calcite and aragonite was calculated from all available data sets. Four selected cross sections, three longitudinal and one latitudinal, and two three-dimensional graphs show that a large volume of the North Pacific is undersaturated with respect to $CaCO_3$. The saturation horizon generally shows a shoaling from west to east and from south to north in the North Pacific Ocean. It was found that the lysocline is at a depth much deeper (about 2500 m deeper) than the saturation horizon of calcite, and several hundred meters shallower than the calcium carbonate compensation depth. Our results appear to support the kinetic point of view of the $CaCO_3$ dissolution mechanisms. Differences in the abundance of the calcareous sediments are explained by differences in the calcium carbonate compensation depth.

Coachman, L.K., and K. AAGAARD. Transports through Bering Strait: annual and interannual variability. *Journal of Geophysical Research* 93(C12):15,535–15,539 (1988).

Reanalysis of the 1976–1977 mean monthly transport estimates for Bering Strait of Coachman and Aagaard (1981) shows a considerably stronger wind dependence than was calculated by Aagaard *et al.* (1985). We find (1) a long-term mean transport of 0.8 Sv, (2) an annual transport cycle of amplitude 0.6 Sv, with the maximum in June, the minimum in February, and a secondary maximum in January probably associated with North Pacific

blocking-ridge activity, and (3) an interannual variability marked by a number of low-flow years in the past two decades, including three of the four lowest-transport winter periods during this century. In a new current time series from 1984 to 1985 we find anomalously strong and persistent northerly flow during a 2-month period in which the current/wind correlation breaks down. This occurred during a prolonged period with southerly winds, and we believe the data point to an asymmetry in the dynamical response of the Bering Strait flow to major changes in wind direction.

CURL, H.C., JR. Marine ecology: the water column. Proceedings of a Conference/Workshop on Recommendations for Studies in Washington and Oregon: Offshore Oil and Gas Development. Minerals Management Service, Dept. of Interior, May 23–25, 1988, Portland, OR, 65–72 (1989).

No abstract.

EBLE, M.C., F.I. GONZALEZ, D.M. MATTENS, and H.B. MILBURN. Instrumentation, field operations, and data processing for PMEL deep ocean bottom pressure measurements. NOAA TM ERL PMEL-89 (NTIS not yet available), 71 pp. (1989).

The focus of this report is on the collection and processing of deep-ocean bottom pressure measurements made using the Paroscientific Model 410K-017 digiquartz pressure transducer. The observational program was initiated in 1986 for the purpose of collecting high quality data during the generation, propagation, and coastal runup stages of a tsunamigenic event. Because of its diversity and flexibility, the bottom pressure recorder (BPR) is also an important tool in many other areas of oceanic research, particularly when coupled with other instrumentation.

EMBLEY, R.W., S.R. HAMMOND, and K. MURPHY. The caldera of Axial Volcano – remote sensing and submersible studies of a hydrothermally active submarine volcano. In *Global Venting, Midwater, and Benthic Ecological Processes*, M.P. De Luca and I. Babb (eds.), National Undersea Research Program Report 88–4, 61–70 (1988).

No abstract.

FEELY, R.A., R.H. Byrne, J.G. Acker, P.R. Betzer, C.T.A. Chen, J.F. GENDRON, and M.F. LAMB. Winter-summer variations of calcite and aragonite saturation in the northeast Pacific. *Marine Chemistry* 25:227–241 (1988).

New carbonate data obtained on February-March and June-July cruises in the northeast Pacific during 1985 were utilized to describe processes affecting seasonal variations of calcite and aragonite saturation. Large gradients in saturation state occur in the region between the Subtropical and the Subarctic Fronts in the north-south direction. These

gradients are a function of large-scale mixing and biological processes in the North Pacific. The saturation values in the upper kilometer of the water column were observed to be significantly lower in winter than in summer. These decreases were due to a number of processes including: (i) the seasonal decrease in the temperature of the water column; (ii) the seasonal increase in vertical mixing causing CO_2-enriched deep waters to be upwelled; and (iii) the seasonal enhancement of respiration over photosynthesis. Seasonal changes in total CO_2 (TCO_2) concentrations appeared to have the greatest overall effect on the saturation state. Aragonite dissolution rate experiments were conducted during the June-July cruise to provide an independent verification of the saturation calculations. In all cases, significant increases in aragonite dissolution were observed below the 100% saturation depth. In the northeast Pacific, shallow undersaturation horizons provide for significant dissolution rates at depths below 400 m.

FOX, C.G. Empirically derived relationships between fractal dimension and power law form frequency spectra. *PAGEOPH* 131(1/2):211–239 (1989).

Fractal analysis and Fourier analysis are independent techniques for quantitatively describing the variability of natural figures. Both methods have been applied to a variety of natural phenomena. Previous analytical work has formulated relationships between the fractal dimension and power law form frequency spectrum. Mandelbrot (1985) has shown that difficulties arise when the ruler method for measuring dimensionality is applied to other than self-similar figures. Since an investigator presumably does not know in advance the dimensionality of a natural profile, it is essential to quantify the nature of the discrepancy for self-affine cases. In this study, a series of experiments are conducted in which discrete random series of specified spectral forms are analyzed using the fractal ruler method. The various parameters of the fractal measurement are related to the parameters of the spectral model. In this way, empirical relationships between the techniques can be derived for discrete, finite series which simulate the results of applying the fractal method to observational data. The results of the study indicate that there are considerable discrepancies between the results predicted by theory and those derived empirically. The fundamental power law form of length versus resolution pairs does not hold over the entire region of analysis. The predicted linear relationship between fractal dimension and exponent of the frequency spectrum does not hold, and the spectral signals can be extended beyond the limits of dimension inferred by theory. Root-mean-square variability is also shown to be linearly related to the fractal intercept term. An investigation of the effect of nonstationary sampling is conducted by generating signals composed of segments of differing spectral characteristics. Fractal analyses of these signals appear identical to those conducted on stationary series. The discrepancies between theoretical prediction and empirical results described in this study reflect the difficulties of applying analytically derived techniques to measurement data. Both Fourier and fractal techniques are formulated through rigorous mathematics, assuming various conditions for the underlying signal. When these techniques are applied to discrete, finite length, nonstationary series, certain statistical transformations must be applied to the data. Methods such as windowing, prewhitening, and anti-aliasing filters have been developed over many years for use with Fourier analysis. At present, no such statistical theory exists for use with fractal analysis. It is apparent from the results of this study that

such a statistical foundation is required before the fractal ruler method can be routinely applied to observation data.

FOX, C.G., and M. VAN HEESWIJK. Sea Beam backscatter analysis applied to the classification of deep-sea volcanic terrains. In *Global Venting, Midwater, and Benthic Ecological Processes*, M.P. De Luca and I. Babb (eds.), National Undersea Research Program Report 88–4, 71–79 (1988).

Hull-mounted sonar systems, such as Sea Beam, are typically used for mapping the bathymetry of the deep-sea floor. The same digital information that is used for the measurement of depth can be evaluated for the backscattering properties of the seafloor. The unique morphologies and petrologies of volcanic and hydrothermal terrains may produce identifiable backscatter signatures. The *Alvin* support vessel *Atlantis* II is equipped for digitally acquiring Sea Beam backscatter energy traces, allowing sonar remote sensing and submersible exploration to be performed in tandem. An experiment funded by the National Undersea Research Program, at Axial Seamount, Juan de Fuca Ridge, has produced the most extensive data set to date from a known hydrothermal area, and these data are being calibrated using the large groundtruth data base collected by NOAA's VENTS research program.

FREITAG, H.P., M.J. MCPHADEN, and A.J. SHEPHERD. Comparison of equatorial winds as measured by cup and propeller anemometers. *Journal of Atmospheric and Oceanic Technology* 6(2):327–332 (1989).

This study compares the performance of cup vs. propeller anemometers from surface-following taut-line moorings in the equatorial Pacific. Vector wind components at 4 m above the sea surface were measured from a mooring instrumented with a cup anemometer and concurrently from a nearby mooring instrumented with a propeller anemometer. Mean wind conditions over the 115–day comparison period were typical of the southeast trade winds with a mean speed of 6.7 m s^{-1} and a steadiness factor of 0.96. Differences between the time series measured by the two wind sensors were small. Mean speed differed by 0.02 m s^{-1} and mean direction by 1.4°. Correlation coefficients for 2-hour vector-averaged zonal component, meridional component, speed and direction were 0.97 or above. The small differences in measurements imply that the two systems are equally suited for near-surface wind observations under typical tradewind conditions.

FREITAG, H.P., M.J. MCPHADEN, and A.J. SHEPHERD. Real-time surface currents from moored buoys. 1989 North American Argos Users Conference and Exhibit, May 15-17, 1989, Service Argos Inc., Landover, MD, 85-100 (1989).

Real-time near surface current and temperature are transmitted via Argos from taut-line moorings in the equatorial Pacific. The moorings are part of EPOCS and TOGA programs to study interannual variability in the wind, current, and temperature fields related to the El

Niño/Southern Oscillation phenomenon. An EG&G Vector Measuring Current Meter at 8 m depth transfers serial data at 2-hour intervals to an Argos transmitter on a surface buoy via a 3-wire conducting cable and interface. Four 2-hour average data values are included in each Argos transmission. This sample rate assures complete daily coverage on the equator. The system is presently incorporated on moorings at 0°, 110°W, 0°, 140°W, and 0°, 165°E which are replaced at 6-month intervals. An independent instrument package on the buoy transmits vector-averaged winds, air and sea-surface temperature. These current meter moorings are a part of a larger network of moorings which cover the equatorial Pacific from 165°E to 110°W.

Giese, B.S. Equatorial oceanic response to forcing on time scales from days to months. NOAA TM ERL PMEL-87 (PB89–206775), 99 pp. (1989).

Episodes of westerly wind in the western Pacific may be an important source of sea surface temperature variability in the eastern Pacific on monthly, seasonal and interannual time scales. In this report we use a combination of data, linear theory and an ocean general circulation model to examine remote response to western Pacific wind forcing. Characteristics of the wind anomaly are determined using daily averaged observations of wind from equatorial islands near the date line. In the model, wind anomalies generate a train of eastward propagating Kelvin pulses. When the wind anomaly is weak the Kelvin response agrees with predictions of linear theory. For more realistic strong forcing there are three important deviations from linear theory; the amplitude of low baroclinic modes increases, the amplitude of higher baroclinic modes decreases, and the phase speed increases. In the presence of realistic oceanic background conditions, response in the equatorial waveguide is complicated by the equatorial undercurrent, a sloping thermocline and instability waves. As Kelvin pulses propagate from western to eastern Pacific surface zonal velocity associated with the first mode decreases, whereas velocity associated with the second mode increases. These changes can be deduced by the principle of conservation of energy flux. In the central and eastern Pacific Kelvin pulses act to amplify and change the phase of existing instability waves. Thermal changes brought about by enlarged instability waves can be comparable in magnitude to changes brought about by zonal advection of the zonal temperature gradient by Kelvin pulses. At the coast of South America, model Kelvin pulses cause a warming of 2°C for 45 days. Current observations made at 140°W and 110°W subsequent to a strong westerly wind event in May 1986 indicate passage of Kelvin-like pulses which agree in magnitude and timing with those modeled. At the coast of South America observations of sea surface temperature show a warm anomaly that lasts for almost two months, comparable in duration and magnitude to changes found in the model.

HARRISON, D.E. Local and remote forcing of ENSO ocean waveguide response. *Journal of Physical Oceanography* 19(5):691–695 (1989).

Several experiments using an ocean general circulation model have been carried out in order to explore the degree to which the oceanic waveguide response during the 1982–83 ENSO event was locally and remotely forced. Experiments in which the chosen monthly mean

surface stress field was imposed only within three degrees of the equator (3°N/S) and within seven degrees of the equator (7°N/S) reveal that the 7°N/S winds reproduce the equatorial results of the full winds case to within differences small compared to the variability of interest. The 3°N/S winds case reproduces equatorial dynamic height acceptably, but introduces errors in SST and upper-ocean currents that approach the ENSO signal. A 7°N-S experiment in which the meridional stress is set to zero (NOYST) shows that meridional stress plays a nontrivial, but not dominant role, in the 1982–83 model behavior; errors generally are comparable to those of the 3°N/S case. A final experiment, in which the 1982–83 winds were imposed west of the dateline and climatological winds were imposed east of 170°W (WPAC), illustrates the extent to which the central and eastern Pacific were forced by winds in the western Pacific. While there is nontrivial remote forcing, the locally forced variability is roughly twice as great. Implications for coupled ocean-atmosphere modeling and for design of future surface wind stress monitoring arrays for ENSO prediction are considered.

HARRISON, D.E. On climatological monthly mean wind stress and wind stress curl fields over the world ocean. *Journal of Climate* 2(1):57–70 (1989).

Using a version of the global surface marine observation historical data set, a new 1° spatial resolution global ocean surface wind stress climatology has been evaluated using the Large and Pond surface drag coefficient formulation. These new results are compared, after spatial smoothing, with those of Hellerman and Rosenstein, who used a different drag coefficient form. It is found that the new stresses are almost everywhere smaller than those of Hellerman and Rosenstein, often by 20%–30%, which is greater than the formal error estimates from their calculations. The stress differences show large-scale spatial structure, as would be expected given the spatial variation of the surface stability parameter and the known different wind variability regions. Basin zonally averaged Ekman transports are computed to provide perspective on the significance of the stress differences; annual mean differences can exceed 10 Sv (Sv ~ 10^6 m^3 s^{-1}) equatorward of 20° lat, but are smaller poleward. Wind stress curl and Sverdrup transport calculations provide a different perspective on the differences; particularly noticeable differences are found in the regions of the Gulf Stream and Kuroshio separation. Large annual variations in midlatitude wind stress curl suggest that study of the forced response at annual periods should be of interest.

HARRISON, D.E., and B.S. Giese. Comment on "The response of the equatorial Pacific Ocean to a westerly wind burst in May 1986" by M.J. McPhaden et al. *Journal of Geophysical Research* 94(C4):5024–5026 (1989).

No abstract.

HARRISON, D.E., W.S. Kessler, and B.S. Giese. Ocean circulation model hindcasts of the 1982–83 El Niño: thermal variability along the ship-of-opportunity tracks. *Journal of Physical Oceanography* 19(4):397–418 (1989).

Five different analyses of 1982–83 monthly average surface wind stress fields have been used to force an ocean general circulation model of the tropical Pacific, in a series of El Niño hindcast experiments, like the one reported by Philander and Seigel. Although there were prominent common departures from climatology in the surface wind stress field during 1982–83 according to each wind analysis, there are also very substantial differences between analyses. This study was done to investigate the sensitivity of such hindcasts to our uncertain knowledge of the surface wind stress field. We concentrate here on the behavior along the Pacific ship-of-opportunity tracks. According to the ship-of-opportunity XBT data, the ocean underwent major changes during this period. The vertical temperature gradients and mixed layer temperatures, as well as the depth of the thermocline, underwent substantial changes. There were also major changes in the geostrophic flow of the major current systems, as revealed by upper ocean dynamic height differences. Comparing the hindcasts with observations, we find that the gross large-scale changes of the ENSO event – surface warming in the second half of 1982, continued warmth into 1983 and cooling in mid-1983, together with major thermocline depth changes – are found in each hindcast. However, major quantitative differences exist between each hindcast and the observations in at least some region for some time and some variable. Within the waveguide, dynamic height changes generally are hindcast with quantitative skill using each wind stress field and the best hindcasts differ from the observations by only a few dyn-cm more than the estimated uncertainty in the observations. Such hindcast skill is unlikely to be fortuitous: evidently the major elements of the waveguide variability are forced by the 1982–83 surface wind stress field rather than evolving out of some aspect of the state of the ocean during late 1981. Sea surface temperature changes are generally hindcast with qualitative skill, but rms errors of 2–3°C are frequent. Subsurface temperature variability skill varies with hindcast, location and depth; skill is greatest in the thermocline. Outside the waveguide, hindcast skill tends to be reduced, and varies greatly with location and hindcast. Quantitative hindcast skill is found near 10°S and 10°N in some hindcasts in the WP, and near 10°S in most hindcasts in the CP, but there is never quantitative skill in the NECC region. The most striking inconsistency found involves the behavior of the NMC hindcast in the region of the North Equatorial Counter Current. Wind stress curl-forced Ekman pumping appears to be a significant factor in the variations in the more successful hindcasts. In almost every comparison, the range of hindcast results brackets the observations, suggesting that the model physics is plausible. Overall, the special research effort wind fields produced better dynamic height results than did the operational wind product fields, but the operational fields produced generally better waveguide SST results. Improved knowledge of the surface wind stress field (and its curl) is a minimum requirement if we are to assess more critically model performance, and to identify needed model improvements.

HAYES, S.P., M.J. MCPHADEN, and A. Leetmaa. Observational verification of a quasi real time simulation of the tropical Pacific Ocean. *Journal of Geophysical Research* 94(C2):2147–2157 (1989).

Time series of upper ocean temperature and currents in the equatorial Pacific simulated by a numerical general circulation model run in nearly real time are compared to observations for the period August 1985 through May 1987. The model was forced by monthly mean wind stress and climatological air-sea heat flux. Comparisons with observations near the equator in the western (165°E), central (140°W), and eastern (110°W) Pacific are discussed. Simulated sea surface temperature (SST) was too cool in the eastern Pacific and too warm in the western Pacific. Largest rms deviations were in the east and exceeded 2°C. On and north of the equator in the eastern Pacific, SST and thermocline depth fluctuations on seasonal and monthly time scales were prominent. South of the equator, seasonal variability dominated. The model simulations often reproduced the amplitude and phase of the seasonal changes but not the higher-frequency variability. Model runs which included monthly assimilation of upper ocean temperature observations were included in the study. None of the comparison time series were incorporated in the assimilation. Inclusion of thermal observations generally improved agreement of simulated and observed time series. This improvement was largely due to reduction in the mean offsets of SST and thermocline depths. Data assimilation did little to improve the month-to-month differences in thermocline depth. In addition, south of the equator in the eastern Pacific, relatively large, systematic intra-month SST deviations occurred. These deviations corresponded to an erroneous heat flux of about 80 W m^{-2} and indicated problems in the simulated upper ocean circulation. Although no velocity data were included in the assimilation, the improved model thermal structure led to improved velocity simulation at some locations. No comparisons indicated large-amplitude spurious velocity variations which could be associated with data assimilation transients.

Hinckley, S., K. BAILEY, J. SCHUMACHER, S. Picquelle, and P. STABENO. Preliminary results of a survey for late-stage larval walleye pollock and observations of larval drift in the western Gulf of Alaska, 1987. In *Proceedings of the International Symposium on the Biology and Management of Walleye Pollock*, Nov. 1988, Anchorage, AK, Alaska Sea Grant Report 89–1, 297–306 (1989).

In June and July of 1987, an exploratory survey for the nursery area of the late-larval and early-juvenile stages of walleye pollock (*Theragra chalcogramma*) was conducted in the western Gulf of Alaska. The goals of the survey were to define the geographical distribution of these life stages, estimate abundance, examine drift to their nursery area, and examine the feasibility of using these life stages in a pre-recruit survey. This paper represents a preliminary report on results of the survey. The center of distribution of late-larval and early-juvenile walleye pollock was between the Shumagin and the Semidi Islands. This corresponded to concurrent locations of satellite-tracked drifters released in the center of the egg distribution in Shelikof Strait in April. Larval numbers were low to the southwest and northeast of the center of distribution and offshore of the 200-m depth contour. Estimated total abundance of late-larval and early-juvenile walleye pollock in the survey area was 9.0×10^{10} individuals.

Huyer, A., R.L. Smith, P.J. STABENO, J.A. Church, and N.J. White. Currents off southeastern Australia: results from the Australian Coastal Experiment. *Australian Journal of Marine and Freshwater Research* 39:245–288 (1989).

The Australian Coastal Experiment was conducted off the east coast of New South Wales between September 1983 and March 1984. The experiment was conducted with arrays of current meters spanning the continental margin at three latitudes (37.5°, 34.5°, and 33.0°S), additional shelf moorings at 29° and 42°S, coastal wind and sea-level measurements, monthly conductivity-temperature-depth probe/expendable bathythermograph (CTD/XBT) surveys, and two satellite-tracked buoys. Over the continental shelf and slope, the alongshore component of the current generally exceeded the onshore component, and the subtidal (<0.6 cpd, cycles per day) current variability greatly exceeded the mean flow. Part of the current variability was associated with two separate warm-core eddies that approached the coast, causing strong (>50 cm sec^{-1}), persistent (>8 days), southward currents over the continental slope and outer shelf. Temperature and geostrophic velocity sections through the eddies, maps of ship's drift vectors and temperature contours at 250 m, and the satellite-tracked drifter trajectories showed that these eddies were similar in structure to those observed previously in the East Australian Current region. Both eddies migrated generally southward. Eddy currents over the shelf and slope were rare at Cape Howe (37.5°S), more common near Sydney (34.5°S), and frequent at Newcastle (33.0°S), where strong northward currents were also observed. Near Sydney, the eddy currents over the slope turned clockwise with depth between 280 and 740 m, suggesting net downwelling there. Repeated CTD sections also indicated onshore transport and downwelling at shallower levels; presumably, upwelling occurred farther south where the eddy currents turned offshore. Periodic rotary currents over the continental slope near Sydney and Newcastle indicated the presence of small cyclonic eddies on the flank of a much larger anticyclonic eddy. Between early October and late January, no strong southward currents were observed over the continental margin near Sydney. Data from this "eddy-free" period were analyzed further to examine the structure and variability of the coastal currents. Much of this variability was correlated with fluctuations in coastal sea-level (at zero lag) and with the wind stress (at various lags). The coherence and phase relationships among current, wind-stress, and sea-level records at different latitudes (determined from spectral analysis and frequency-domain empirical orthogonal functions) were consistent with the equatorward propagation of coastal-trapped waves generated by winds in phase with those near Cape Howe. Time-domain empirical orthogonal functions show that the current fluctuations decayed with distance from shore and with depth, as expected of coastal-trapped waves.

Incze, L.S., A.W. Kendall, Jr., J.D. SCHUMACHER, and R.K. REED. Interactions of a mesoscale patch of larval fish (*Theragra chalcogramma*) with the Alaska Coastal Current. *Continental Shelf Research* 9(3):269–284 (1989).

Walleye pollock, *Theragra chalcogramma*, form dense aggregations during a brief spawning period from late March to mid-April in Shelikof Strait, Alaska. Spawning produces a large

(order 20 × 50 km or more) "patch" of eggs at depth (generally >150 m), and hatching larvae often produce a "patch" in the upper 50 m. Patches can be defined as coherent features using graded concentration isopleths, and the mean concentration within patches has been observed to be as much as 68 times (for eggs) and nearly 6 times (for larvae) the background concentration. Larval patches drift southwestward and have been identified for about 30 days after hatching in some years. Data are presented for spawner biomass and for early life stages, as available, for 1981, 1983 and 1985. When comparing 1985 with 1981 (2 years with the best coverage), spawner biomass and mean egg concentration within the patch declined concordantly. Larval concentrations about 10 days after hatching differed widely, however: concentrations in early May 1985 were more than an order of magnitude lower than expected. Unlike either 1981 or 1983, no larval patch could be identified in late May 1985; this appears to be attributable to changes detected earlier in the month. The "apparent" mortality rate for a 10-day period after hatching in 1985 was about 0.50 d^{-1} greater than in 1981. Larval feeding conditions can be excluded as a likely cause of this interannual difference, but predation and advection cannot be. Our findings emphasize the short time period over which significant changes can occur, as well as additional sampling which must be done in future studies. We show that part of the emerging 1985 larval year class could have been removed by cross-channel disturbances in the flow field through Shelikof Strait.

KESSLER, W.S. Observations of long Rossby waves in the northern tropical Pacific. NOAA TM ERL PMEL-86 (PB89–196331), 169 pp. (1989).

Long baroclinic Rossby waves are potentially important in the adjustment of the tropical Pacific pycnocline to both annual and interannual wind stress curl fluctuations. Evidence for such waves is found in variations of the depth of the 20°C isotherm in the northern tropical Pacific during 1970 through 1987. 190,000 bathythermograph profiles have been compiled from the archives of several countries; the data coverage is dense enough that westward-propagating events may be observed with a minimum of zonal interpolation. After extensive quality control, 20°C depths were gridded with a resolution of 2° latitude, 5° longitude and bimonths; statistical parameters of the data were estimated. A simple model of low-frequency pycnocline variability allows the physical processes of Ekman pumping, the radiation of long (non-dispersive) Rossby waves due to such pumping in mid-basin, and the radiation of long Rossby waves from the observed eastern boundary pycnocline depth fluctuations. Although the wind stress curl has very little zonal variability at the annual period in the northern tropical Pacific, an annual fluctuation of 20°C depth propagates westward as a long Rossby wave near 4°–6°N and 14°–18°N in agreement with the model hindcast. Near the thermocline ridge at 10°N, however, the annual cycle is dominated by Ekman pumping. The wave-dominated variability at 4°–6°N weakens the annual cycle of Countercurrent transport in the western Pacific. El Niño events are associated with westerly wind anomalies concentrated in the central equatorial Pacific; an upwelling wind stress curl pattern is generated in the extra-equatorial tropics by these westerlies. Long upwelling Rossby waves were observed to raise the western Pacific thermocline well outside the equatorial waveguide in the later stages of El Niños, consistent with the simple long-wave model. It has been suggested that El Niño events are initiated by downwelling long Rossby waves in the extra-equatorial region reflecting off the western boundary as equatorial Kelvin

waves. The bathythermograph observations show that although such downwelling waves commonly arrive at the western boundary (the Philippines coast), there is a low correlation between these occurrences and the subsequent initiation of El Niño events.

LACKMANN, G.M., and J.E. OVERLAND. Atmospheric structure and momentum balance during a gap-wind event in Shelikof Strait, Alaska. *Monthly Weather Review* 117:1817–1833 (1989).

Gap winds occur in topographically restricted channels when a component of the pressure gradient is parallel to the channel axis. Aircraft flight-level data are used to examine atmospheric structure and momentum balance during an early spring gap-wind event in Shelikof Strait, Alaska. Alongshore sea level pressure ridging was observed. Vertical cross sections show that across-strait gradients of boundary-layer temperature and depth accounted for the pressure distribution. Geostrophic adjustment of the mass field to the along-strait wind component contributed to development of the observed pressure pattern. Boundary-layer structure and force balance during this event was similar to that often observed along isolated barriers. However, the Rossby radius was larger than the strait width, and atmospheric structure in the strait exit region indicates transition of the flow to open coastline conditions. Two across-strait momentum budgets show that the Coriolis force and across-strait pressure gradient were an order of magnitude larger than other terms. Largest terms in the along-strait balance were the pressure gradient force, acceleration, entrainment, and friction. Boundary-layer acceleration in the along-strait direction was 55% of the potential limit determined by the along-strait pressure gradient. Entrainment of air into the boundary layer was the largest retarding force and contributed to the along-strait profile of boundary-layer depth. Large horizontal divergence was observed within the strait, yet boundary-layer depth increased slightly following the flow. Entrainment at the inversion and sea surface fluxes accounted for along-strait variation of boundary-layer equivalent potential temperature.

LAVELLE, J.W., H.O. MOFJELD, E. LEMPRIERE-DOGGETT, G.A. CANNON, D.J. PASHINSKI, E.D. COKELET, L. LYTLE, and S. Gill. A multiply-connected channel model of tides and tidal currents in Puget Sound, Washington and a comparison with updated observations. NOAA TM ERL PMEL-84 (PB89–139786), 103 pp. (1989).

Tides and tidal transports within Puget Sound have been calculated using a model in which the Sound is represented by 79 channels connected at 43 junctions. Linearized equations of motion were used to determine channel cross-sectionally averaged quantities for the principal tidal constituents (M_2, K_1, S_2, N_2, O_1, P_1, M_4). For the M_2 tide the amplitudes and phases at the entrances to the Sound and the friction coefficients in the channels were adjusted to bring observed and modeled tidal distributions into best agreement; for other constituents, only the tidal amplitudes and phases at the entrances were adjusted. Data from 47 tide stations in Puget Sound were used for fitting model parameters. Tidal amplitudes and phases match observations with an average difference of less than 1 cm and 2° respectively for each of the constituents indicated. Transport values from the model were subse-

(order 20 × 50 km or more) "patch" of eggs at depth (generally >150 m), and hatching larvae often produce a "patch" in the upper 50 m. Patches can be defined as coherent features using graded concentration isopleths, and the mean concentration within patches has been observed to be as much as 68 times (for eggs) and nearly 6 times (for larvae) the background concentration. Larval patches drift southwestward and have been identified for about 30 days after hatching in some years. Data are presented for spawner biomass and for early life stages, as available, for 1981, 1983 and 1985. When comparing 1985 with 1981 (2 years with the best coverage), spawner biomass and mean egg concentration within the patch declined concordantly. Larval concentrations about 10 days after hatching differed widely, however: concentrations in early May 1985 were more than an order of magnitude lower than expected. Unlike either 1981 or 1983, no larval patch could be identified in late May 1985; this appears to be attributable to changes detected earlier in the month. The "apparent" mortality rate for a 10-day period after hatching in 1985 was about 0.50 d^{-1} greater than in 1981. Larval feeding conditions can be excluded as a likely cause of this interannual difference, but predation and advection cannot be. Our findings emphasize the short time period over which significant changes can occur, as well as additional sampling which must be done in future studies. We show that part of the emerging 1985 larval year class could have been removed by cross-channel disturbances in the flow field through Shelikof Strait.

KESSLER, W.S. Observations of long Rossby waves in the northern tropical Pacific. NOAA TM ERL PMEL-86 (PB89–196331), 169 pp. (1989).

Long baroclinic Rossby waves are potentially important in the adjustment of the tropical Pacific pycnocline to both annual and interannual wind stress curl fluctuations. Evidence for such waves is found in variations of the depth of the 20°C isotherm in the northern tropical Pacific during 1970 through 1987. 190,000 bathythermograph profiles have been compiled from the archives of several countries; the data coverage is dense enough that westward-propagating events may be observed with a minimum of zonal interpolation. After extensive quality control, 20°C depths were gridded with a resolution of 2° latitude, 5° longitude and bimonths; statistical parameters of the data were estimated. A simple model of low-frequency pycnocline variability allows the physical processes of Ekman pumping, the radiation of long (non-dispersive) Rossby waves due to such pumping in mid-basin, and the radiation of long Rossby waves from the observed eastern boundary pycnocline depth fluctuations. Although the wind stress curl has very little zonal variability at the annual period in the northern tropical Pacific, an annual fluctuation of 20°C depth propagates westward as a long Rossby wave near 4°–6°N and 14°–18°N in agreement with the model hindcast. Near the thermocline ridge at 10°N, however, the annual cycle is dominated by Ekman pumping. The wave-dominated variability at 4°–6°N weakens the annual cycle of Countercurrent transport in the western Pacific. El Niño events are associated with westerly wind anomalies concentrated in the central equatorial Pacific; an upwelling wind stress curl pattern is generated in the extra-equatorial tropics by these westerlies. Long upwelling Rossby waves were observed to raise the western Pacific thermocline well outside the equatorial waveguide in the later stages of El Niños, consistent with the simple long-wave model. It has been suggested that El Niño events are initiated by downwelling long Rossby waves in the extra-equatorial region reflecting off the western boundary as equatorial Kelvin

waves. The bathythermograph observations show that although such downwelling waves commonly arrive at the western boundary (the Philippines coast), there is a low correlation between these occurrences and the subsequent initiation of El Niño events.

LACKMANN, G.M., and J.E. OVERLAND. Atmospheric structure and momentum balance during a gap-wind event in Shelikof Strait, Alaska. *Monthly Weather Review* 117:1817–1833 (1989).

Gap winds occur in topographically restricted channels when a component of the pressure gradient is parallel to the channel axis. Aircraft flight-level data are used to examine atmospheric structure and momentum balance during an early spring gap-wind event in Shelikof Strait, Alaska. Alongshore sea level pressure ridging was observed. Vertical cross sections show that across-strait gradients of boundary-layer temperature and depth accounted for the pressure distribution. Geostrophic adjustment of the mass field to the along-strait wind component contributed to development of the observed pressure pattern. Boundary-layer structure and force balance during this event was similar to that often observed along isolated barriers. However, the Rossby radius was larger than the strait width, and atmospheric structure in the strait exit region indicates transition of the flow to open coastline conditions. Two across-strait momentum budgets show that the Coriolis force and across-strait pressure gradient were an order of magnitude larger than other terms. Largest terms in the along-strait balance were the pressure gradient force, acceleration, entrainment, and friction. Boundary-layer acceleration in the along-strait direction was 55% of the potential limit determined by the along-strait pressure gradient. Entrainment of air into the boundary layer was the largest retarding force and contributed to the along-strait profile of boundary-layer depth. Large horizontal divergence was observed within the strait, yet boundary-layer depth increased slightly following the flow. Entrainment at the inversion and sea surface fluxes accounted for along-strait variation of boundary-layer equivalent potential temperature.

LAVELLE, J.W., H.O. MOFJELD, E. LEMPRIERE-DOGGETT, G.A. CANNON, D.J. PASHINSKI, E.D. COKELET, L. LYTLE, and S. Gill. A multiply-connected channel model of tides and tidal currents in Puget Sound, Washington and a comparison with updated observations. NOAA TM ERL PMEL-84 (PB89–139786), 103 pp. (1989).

Tides and tidal transports within Puget Sound have been calculated using a model in which the Sound is represented by 79 channels connected at 43 junctions. Linearized equations of motion were used to determine channel cross-sectionally averaged quantities for the principal tidal constituents (M_2, K_1, S_2, N_2, O_1, P_1, M_4). For the M_2 tide the amplitudes and phases at the entrances to the Sound and the friction coefficients in the channels were adjusted to bring observed and modeled tidal distributions into best agreement; for other constituents, only the tidal amplitudes and phases at the entrances were adjusted. Data from 47 tide stations in Puget Sound were used for fitting model parameters. Tidal amplitudes and phases match observations with an average difference of less than 1 cm and 2° respectively for each of the constituents indicated. Transport values from the model were subse-

quently compared to transports calculated from currents measured on four sections across the Sound at both M_2 and K_1 frequencies. Tidal transports at the M_2 frequency match the transports calculated from the data with average difference of less than 3% for amplitude and 4.3° for phase. The model was also used to calculate cross-sectionally averaged tidal currents, tidal prisms, and tidal dissipation rates for the composite tide and for constituents. As an example of those results, the composite tide and the M_2 and K_1 constituents have tidal prisms of 7.69, 4.74 and 3.73 km^3 and dissipation rates of 733,528 and 78 MW, respectively.

Lupton, J.E., E.T. BAKER, and G.J. MASSOTH. Variable ^{3}He/heat ratios in submarine hydrothermal systems: evidence from two plumes over the Juan de Fuca ridge. *Nature* 337(6203):161–164 (1989).

The first vent fluid samples recovered from submarine hydrothermal systems on the Galápagos Rift and at 21°N on the East Pacific Rise (EPR) had a nearly identical ratio of ^{3}He/heat of ~0.5×10^{-12} cm^3 STP cal^{-1}, even though the two hydrothermal systems were separated geographically and had widely differing fluid exit temperatures (~20 and ~350°C, respectively). Jenkins *et al.* combined this ratio with independent estimates of the flux of mantle ^{3}He through the oceans, to calculate a global oceanic hydrothermal heat flux of 4.9×10^{19} cal yr^{-1}, which is in excellent agreement with geophysical estimates for this flux. Other investigators then combined this ^{3}He flux with measured ratios of various chemicals in vent fluids to ^{3}He (such as Mn/^{3}He and Si/^{3}He) to estimate global hydrothermal fluxes for these species. Here we show that ^{3}He/heat ratios vary by over an order of magnitude between submarine hydrothermal systems, suggesting that early measurements of the ^{3}He/heat relation are not representative of all hydrothermal systems, and that flux calculations based on the oceanic ^{3}He flux must be undertaken with caution.

MASSOTH, G.J., D.A. Butterfield, J.E. Lupton, R.E. McDuff, M.D. Lilley, and I.R. Jonasson. Submarine venting of phase-separated hydrothermal fluids at Axial Volcano, Juan de Fuca Ridge. *Nature* 340:702–705 (1989).

Since the discovery of high-temperature venting on the East Pacific Rise in 1979, it has been expected, because of the physical properties of sea water at pressures and temperatures encountered during submarine hydrothermal circulation, that phase-separated fluids would discharge from ridgecrest vents. Although this notion is supported by the reported large deviations in vent-fluid chlorinity relative to that of sea water (–40% – +200%), by observations of venting at P-T conditions clearly within the two-phase region (220 bar and 420°C) and by fluid-inclusion data, unequivocal identification of phase-separated venting fluids has remained elusive. Here we report observations of chloride- and metal-depleted, gas-enriched fluids from a shallow vent field on the Juan de Fuca Ridge which confirm the expectation that phase-separated effluents are delivered to the deep ocean from some sea-floor venting systems.

MASSOTH, G.J., H.B. MILBURN, S.R. HAMMOND, D.A. Butterfield, R.E. McDuff, and J.E. Lupton. The geochemistry of submarine venting fluids at Axial Volcano, Juan de Fuca Ridge: new sampling methods and a VENTS Program rationale. In *Global Venting, Midwater and Benthic Ecological Processes*, M.P. De Luca and I. Babb (eds.), National Undersea Research Program Report 88–4, 29–59 (1988).

Observations of vent fluids collected in 1986 with the submersible *Pisces* IV from the ASHES vent field at Axial Volcano, Juan de Fuca Ridge suggest that hydrothermal fluids similar to those vented at other sediment-starved ridgecrest sites are being discharged along with unprecedented Cl-poor, gas-enriched fluids that are likely the result of phase separation. Anomalously low concentrations of silica, calcium, manganese and iron were also observed in the Cl-poor vent fluids. New sampling tools and protocols conceived to overcome the interpretive limitations inherent to conventional vent fluid data were tested during 1987 using the Deep Submersible *Alvin*. A Submersible-coupled *In situ* Sensing and Sampling System (SIS^3) enabled a more efficient collection of high quality vent fluid samples coincident with the sensing of temperature. An *In Situ* Chemical Analyzer (ISCA), based on the technology of flow injection analysis and configured to monitor the chemical output of a warm spring vent for H_2S, Fe^{2+}, pH, and temperature, was deployed with partial success for 3 days at the ASHES vent field. The integral role of vent fluid studies in testing the hypothesis that hydrothermal venting along the Juan de Fuca/Explorer/Gorda Ridge system plays a major role in controlling the chemistry of the northeastern Pacific Ocean is identified and supported.

MCPHADEN, M.J., and R.A. Fine. A dynamical interpretation of the tritium maximum in the central equatorial Pacific. *Journal of Physical Oceanography* 18(10):1454–1457 (1988).

The tropical tritium distribution between 1974 and 1981 is characterized by a maximum along the equator centered between 125° and 145°W. It signifies that this region has received the maximum input of high northern latitude water. A dynamical interpretation of the maximum shows that it can be explained by the strength of the Sverdrup circulation in the central equatorial Pacific where there is a strong zonal convergence in the North Equatorial Countercurrent (NECC) and a strong meridional geostrophic flow towards the equator.

MCPHADEN, M.J., H.P. FREITAG, S.P. HAYES, B.A. TAFT, Z. Chen, and K. Wyrtki. Reply to Comment by Harrison and Giese. *Journal of Geophysical Research* 94(C4):5027–5028 (1989).

No abstract.

MCPHADEN, M.J., and B.A. TAFT. Dynamics of seasonal and intraseasonal variability in the eastern equatorial Pacific. *Journal of Physical Oceanography* 18(11):1713–1732 (1988).

Time series measurements from surface moored buoys in the eastern equatorial Pacific are analyzed for the period 1983–86. The data, collected as part of the EPOCS and TROPIC HEAT programs, consist of currents, temperatures, and winds on the equator at 110°, 124.5° and 140°W. The purpose is to examine the dynamics of seasonal and intraseasonal variability in the upper 250 m from a diagnosis of the depth integrated zonal momentum (i.e., transport) equation. The principal conclusions of this paper are that 1) there is an approximate balance between mean zonal wind stress and depth integrated pressure gradient; nonlinear advection is significantly nonzero however and leads to an enhancement of eastward transport along the equator; 2) there is an interannual change in zonal wind stress and pressure gradient in which both approximately double over the record length; 3) at the annual cycle, zonal wind stress and depth integrated pressure gradient tend to balance, though the uncertainties are large and other physical processes (e.g., lateral diffusion) are likely to be important; and 4) there exists a very energetic intraseasonal eastward propagating Kelvin-like wave in zonal current, temperature, and dynamic height at periods of 60–90 days which is poorly correlated with the local winds. These waves have amplitudes that are large enough at times to obscure the annual cycle.

MOFJELD, H.O. Depth dependence of bottom stress and quadratic drag coefficient for barotropic pressure-driven currents. *Journal of Physical Oceanography* 18(11), 1658–1669 (1988).

A level 2° turbulence closure model is used to investigate the dependence on water depth H of bottom stress τ_b and quadratic drag coefficient C_d for a steady barotropic pressure-driven current in unstratified water when the current is the primary source of turbulence. For spatially uniform pressure gradient and bottom roughness z_0 the magnitude $|\tau_b|$ increases from small values in shallow water to a maximum (at a depth ~0.004 U_0/f where U_0 is the geostrophic current speed derived from the pressure gradient and f is the Coriolis parameter) at which the dynamics changes from being depth-limited to being controlled by similarity scales. As the depth increases further, $|\tau_b|$ decreases to its deep-water value, that is, 15% to 19% less than the maximum. The angle θ of the bottom stress relative to the geostrophic direction decreases rapidly from 90° in very shallow water, reaching its deep-water value (~11°–21°) at a somewhat shallower depth than does $|\tau_b|$. At the maximum stress θ is 8° larger than the deep-water angle. A set of computationally efficient formulas matched to the model results gives $|\tau_b|$ and θ for all combinations of U_0, H, f and bottom roughness z_0. Comparison with a variety of other models satisfying Rossby similarity over oceanographic ranges of parameters shows agreement of ~10% for $|\tau_b|$ and ~5° for θ. The coefficient C_d of the quadratic drag law relating $|\tau_b|$ to the vertically averaged velocity is found to be approximated reasonably well by a formula from nonrotating channel theory in which the coefficient depends only on the ratio H/z_0. The direction of the bottom stress relative to the vertically averaged velocity is equal to the geostrophic veering angle (~11°–21°) in deep water and decreases to ~5° for a range of intermediate depths (~0.004–0.01 U_0/f) where it is relatively independent of external Rossby number U_0/fz_0; the angle becomes less in shallower water.

Muench, R.D. The sea ice margins: a summary of physical phenomena. NOAA TM ERL PMEL–88 (PB89–212328), 51 pp. (1989).

No abstract.

MURPHY, P.P., T.S. BATES, H.C. CURL, JR., R.A. FEELY, and R.S. BURGER. The transport and fate of particulate hydrocarbons in an urban fjord-like estuary. *Estuarine, Coastal and Shelf Science* 27:461–482 (1988).

Hydrocarbon concentrations were measured on suspended particulates and on surficial marine sediments in the urban fjord-like estuary of Puget Sound, Washington. These data were combined with sediment deposition rates, suspended particulate concentrations and circulation data to assess hydrocarbon distributions and fates. Evaluation of major sinks for petroleum hydrocarbons (UCM) and polycyclic aromatic hydrocarbons (PAH) in an urban estuary indicates that >90% of the hydrocarbons which are associated with suspended particulates in the main basin of Puget Sound are deposited in the estuarine sediments. Approximately 63% of the PAH and 100% of the UCM associated with particles in the main basin settle directly to the sediments. The remainder is carried to the main basin sediments via horizontal transport from other areas. Trends in PAH ratios are used to identify major sources of PAH. Estimated sources of PAH are balanced by the estimated sinks.

Nakata, K., K. Tsurusaki, Y. Okayama, and J.W. LAVELLE. An attempt to evaluate the effects of an anti-turbidity system on sediment dispersion from a Hopper dredge. NOAA TM ERL PMEL–85 (PB89–162515), 30 pp. (1989).

Measurements were made during six hopper dredge operations to investigate the differences in plumes of overspilled particulates when the dredger was and was not using an anti-turbidity system. Observations for discharge rates of suspended solids were taken aboard the dredge ship while concentration samples of suspended solids were taken by survey boats in the plume and currents were metered by instruments on moorings. Measurements were given a common framework by the use of a dispersion model for the plume. Modeled and observational profiles match well when the rate of discharge is reserved as a fitting parameter. However, differences in results of the use and non-use of the anti-turbidity system are not discernible with the field data. Consequently, the model was used under identical advection and diffusion conditions to study the differences theoretically. Those numerical experiments suggest that there is an increase of about 25% in the amount of deposition in the immediate area of dredging with the anti-turbidity system, though the fractional amount of redeposition in both cases is small. The differences in results for the two systems calculated with the model depend on the assigned initial vertical distributions. Because these are poorly known at present, better definition of the differences with and without the anti-turbidity system await better measurements of the vertical distributions of suspended solids in the ocean immediately following discharge.

OVERLAND, J.E., and C.H. PEASE. Modeling ice dynamics of coastal seas. *Journal of Geophysical Research* 93(C12):15,619–15,637 (1988).

A coupled sea ice, barotropic ocean model with a 1-km resolution and a seaward domain of 200 km quantifies three coastal processes: coupling of ice motion to wind-driven coastal currents, ice thickness redistribution under compaction at the coast, and formation of coastal shear zones. The model consists of an ice momentum balance, mass concentration and two-parameter ice thickness distribution, and equations for horizontal water motion and continuity using vertical structure functions. An appropriate constitutive law appears to be a hardening plastic based on qualitative observations from Alaskan continental shelves. For first-year sea ice, strength is taken to be proportional to the square of ice thickness. A north wind example of 10 m/s with the coastline to the west shows the depth dependence of rotational shear in the sea ice/ocean boundary layer and sea surface tilt which contributes an alongshore slope current. There is slight convergence of sea ice over the shelf, a coastal shear zone of 4 km, and an alongshore ice speed seaward of the shear zone of 6% of the wind speed caused by the combination of an under-ice shear layer and an alongshore slope current. For an onshore wind, ice is near free drift at 3% of the wind seaward of a ridging front, which propagates seaward. A square dependence of ice strength on thickness is required for the rubble field to approach a limiting thickness, consistent with observations. The hardening plastic interpretation of the rubble field has the stress state at the yield limit in contrast with a rigid plastic of high constant strength that yields only at the coast. We conclude that (1) ice thickness/motion feedback is important on scales less than 10 km, (2) the observational base to discriminate between mesoscale constitutive laws is not yet available, and (3) the relation of ice velocity to wind stress is variable because the ocean slope current responds only to the alongshore component of the wind.

OVERLAND, J.E., and C.H. PEASE. Prediction of vessel icing: a 1989 update. Proceedings, 10th International Conference on Port and Ocean Engineering Under Arctic Conditions, June 12–16, 1989, Luleå, Sweden, K.B.E. Axelsson and L.A. Fransson (eds.), Luleå University of Technology, Research Report TULEA 1989:08, Vol. 2, 712–723 (1989).

The NOAA vessel icing algorithm is evaluated against theoretical advances. The most difficult factor is influence of sea temperature. Modeling demonstrates the importance of supercooling of spray during its trajectory to extreme ice accretion. This occurs when sea temperatures are less than 2–3°C above the saltwater freezing point. The sea surface temperature term in the NOAA algorithm is consistent with the supercooling hypothesis and a further category of "extreme" icing is added, which can explain anecdotal cases greater than 5 cm h^{-1}. A wave height/wind speed threshold is 5 m s^{-1} for a 15-m vessel, 10 m s^{-1} for a 50-m large trawler and 15 m s^{-1} for a 100-m vessel, developed from seakeeping theory. These wind speeds are exceeded 83%, 47% and 15% during February in the Bering Sea.

PAULSON, A.J., R.A. FEELY, H.C. CURL, JR., E.A. Crecelius, and G.P. Romberg. Separate dissolved and particulate trace metal budgets for an estuarine system: an aid for management decisions. *Environmental Pollution* 57:317–339 (1989).

The sources and sinks of dissolved and particulate Pb, Cu and Zn were determined for the main basin of Puget Sound to understand the effect man has had on metal concentrations in both the water column and in the sediments. Municipal, industrial and atmospheric sources contributed about 66% of the total Pb added to the main basin of Puget Sound during the early 1980s. Advective inputs were the major sources of total Cu and Zn (~40%) while riverine and erosional sources contributed about 30%. The discharge of the particle-bound trace metals from rivers minimized the influence of particulate anthropogenic sources, which constituted 50%, 23% and 18% of the total particulate Pb, Cu and Zn inputs, respectively. While advective transport was the major source of dissolved Cu and Zn (~60% of all dissolved inputs), industrial, municipal and atmospheric inputs contributed about 85%, 30% and 38% of the dissolved Pb, Cu and Zn inputs, respectively. The sources of dissolved and particulate Cu and Zn were comparable with the sinks within the errors of the analyses indicating their quasi-conservative nature. Advection removed about 60% of the total Cu and Zn added to the main basin while 40% was deposited in the sediments of Puget Sound. Because of this quasi-conservative nature of Cu and Zn, anthropogenic inputs of Cu and Zn were dispersed from the system more than they were contained within main basin sediments. About 75% of the dissolved Pb discharged into the main basin of Puget Sound was lost from the dissolved phase and was balanced by a similar gain in the particulate phase. Because of this extensive scavenging and the effective retention of particles within the main basin, about 70% of the total Pb added to the main basin was retained within its sediments. These separate mass balances have utility in management decisions because they show the relative contributions from different sources and demonstrate whether the influences of dissolved and particulate inputs are reflected solely in the water column or the sediments, respectively.

PAULSON, A.J., R.A. FEELY, H.C. CURL, JR., and D.A. TENNANT. Estuarine transport of trace metals in a buoyant riverine plume. *Estuarine, Coastal and Shelf Science* 28:231–248 (1989).

The distributions of dissolved and particulate trace metals in Elliott Bay, Washington were determined in April, 1985 during the period of maximum discharge of freshwater for the year. The high freshwater discharge generated a thin buoyant plume (<2 m) which carried a high suspended load. Calculations made from high resolution sampling of salinity and total suspended matter in the plume suggest that their residence times in the upper 2 m of the water column ranged between 15 and 24 h. Total suspended matter, dissolved and particulate Fe, Mn and Pb, and particulate Cu and Zn in the plume were found to be conservative during their transit through Elliott Bay. Dissolved Cu and Zn exhibited a linear relationship with salinity downstream of a significant anthropogenic source. The particulate phase dominated the horizontal transport of Fe and Pb originating from freshwater sources. In contrast, the dissolved phase contributed 66%, 75% and 35% of the respective total horizontal fluxes of Mn, Zn and Cu that originated from riverine and anthropogenic sources. The trace metal concentrations of the suspended matter were uniform in Elliott Bay except for

Mn concentrations. Mn concentrations of suspended matter increased with salinity due to mixing of lower concentration, riverine particulates with Puget Sound particulates of higher Mn concentrations. The lack of trace metal enrichments of Elliott Bay surface suspended matter during this period of high discharge was the result of the small vertical loss of suspended matter (<2% of the horizontal transport) and the rapid transit of suspended matter through the Bay.

PAULSON, A.J., T.P. Hubbard, H.C. CURL, JR., R.A. FEELY, T.E. Sample, and R.G. Swartz. Decreased fluxes of Pb, Cu and Zn from Elliott Bay. Proceedings of Sixth Symposium on Coastal and Ocean Management/ASCE, July 11–14, 1989, Charleston, SC, 3916–3930 (1989).

Fluxes of dissolved Pb, Cu and Zn to Elliott Bay, Washington from industrial sources were calculated from metal-salinity plots and freshwater discharge rates. The changes in these calculated fluxes were used to evaluate the effectiveness of pollution abatement programs. Between 1981 and 1985, initial pollution abatement actions were directed at many commercial and industrial dischargers along the Duwamish Waterway and on Harbor Island including a secondary lead smelter site and shipbuilding facilities. Subsequently, the dissolved Pb flux to Elliott Bay from industrial flux of dissolved Cu decreased by a factor of 5, and the industrial flux of dissolved Zn remained unchanged. The closure of one shipyard, reduced activity at another and better management practices decreased the industrial fluxes of dissolved Cu and Zn to Elliott Bay in 1986 by 75% and 90%, respectively.

PEASE, C.H. Beaufort/Chukchi ice motion and meteorology update. Proceedings, Alaska OCS Region 1987 Arctic Information Transfer Meeting Conference, OCS Study MMS 88–0040, Minerals Management Service, Anchorage, AK, 145–150 (1988).

No abstract.

Picaut, J., S.P. HAYES, and M.J. MCPHADEN. Use of the geostrophic approximation to estimate time varying zonal currents at the equator. *Journal of Geophysical Research* 94(C3):3228–3236 (1989).

Moored thermistor chains at 2°N and 2°S and current-temperature moorings at 0° are used to examine the accuracy of geostrophically estimated zonal velocity on the equator in the eastern (110°W) and western (165°E) Pacific. The meridionally differentiated form of the geostrophic balance is used to eliminate large errors due to wind-balanced cross-equatorial pressure gradients. Statistical analyses indicate that for time scales longer than 30–50 days, the observed and geostrophically estimated zonal velocities are similar (correlation coefficients of 0.6–0.9 and comparable amplitudes). Thus low-frequency equatorial current oscillations are reasonably well represented by the geostrophic approximation. However, the mean currents are poorly resolved with the available array. In the eastern Pacific the mean zonal speed difference over the 10-month comparison period is 25 cm s^{-1} at 25 m and increases to 60 cm s^{-1} at 125 m. At 165°E mean differences in the upper 250 m are typically

50 cm s^{-1} over a 4-month record. The principal reason for these large mean differences is that the meridional scale of the mean currents is smaller than the spacing of the moorings. Comparison of observed and geostrophic velocity profiles obtained from shipboard sampling indicates that meridional spacing of about 1° latitude would be optimum for estimating the zonal velocity.

QUINN, P.K., and T.S. BATES. Collection efficiencies of a tandem sampling system for atmospheric aerosol particles and gaseous ammonia and sulfur dioxide. *Environmental Science and Technology* 23(6):736–739 (1989).

The collection efficiencies of aerosol particles and gaseous NH_3 and SO_2 were tested for a tandem sampling system consisting of a cyclone separator followed by a 1.0 μm pore size 47-mm Millipore Teflon particle filter and four 47-mm Whatman 41 filters coated with oxalic acid and either K_2CO_3 or LiOH. The collection efficiency of the cyclone was compared with an 8.0 μm pore size Nuclepore filter using NaCl particles. Both the cyclone and the filter had a 50% collection efficiency at 0.9 μm (50 standard L/min, 55 cm s^{-1} filter face velocity). Known amounts of NH_3 and SO_2 were generated and collected on the coated filters. The collection efficiency of the system for NH_3 was found to be 103 ± 30%. The SO_2 collection efficiency on K_2CO_3- and LiOH-coated filters was 100 ± 21 and 88 ± 9%, respectively, and was not affected by the presence of reduced sulfur gases or ozone in the sampled air stream.

REED, R.K. and J.D. SCHUMACHER. Some mesoscale features of flow in Shelikof Strait, Alaska. *Journal of Geophysical Research* 94(C9):12,603–12,606 (1989).

Moored current observations were obtained from a small region of Shelikof Strait during 1986–1987. Results from two sites <4 km apart revealed very similar energy spectra and highly correlated alongstream component flow. At separations >11 km, however, correlations were quite weak. A new feature, intense 13-day spectral peaks of narrow horizontal and vertical scale, was also revealed. The feature appears to be a baroclinic, residual flow linked to tidal currents.

REED, R.K., and J.D. SCHUMACHER. Transport and physical properties in central Shelikof Strait, Alaska. *Continental Shelf Research* 9(3):261–268 (1989).

Data from a repeated CTD section in central Shelikof Strait during 1985–1987 are used to derive volume transport and the distribution of near-bottom physical properties. Mean transport was 0.6×10^6 m^3 s^{-1} to the southwest, similar to that measured by a 5-month current-meter array. Computed transport values varied from 0.2 to 1.2×10^6 m^3 s^{-1}; differential Ekman pumping appeared to be important in creating large changes in transport over short time intervals. Near-bottom temperature and salinity varied as a result of changes in source waters to the south; during 1986 cold, low-salinity conditions prevailed. The

seasonal cycles of surface and near-bottom temperature and salinity are compared to those found off the Kenai Peninsula.

REED, R.K., J.D. SCHUMACHER, and A.W. Kendall, Jr. NOAA's Fisheries Oceanography Coordinated Investigations in the Western Gulf of Alaska. *Eos, Transactions American Geophysical Union: The Oceanography Report* 69(40):890–894 (1989).

No abstract.

Reynolds, R.W., K. Arpe, C. Gordon, S.P. HAYES, A. Leetmaa, and M.J. MCPHADEN. A comparison of tropical Pacific surface wind analyses. *Journal of Climate* 2(1):105–111 (1989).

Surface wind analyses from three data assimilation systems are compared with independent wind observations from six buoys located in the Pacific within 8 deg of the equator. The period of comparison is 6 months (February to July 1987), with daily sampling. The agreement between the assimilation systems and the independent buoy data is disappointing. The long-term mean differences between the buoy and the assimilated zonal and meridional winds are as large as 3.1 m s^{-1}, which is comparable to the size of the means themselves. The zonal and meridional daily wind correlations range between 0.66 and 0.17. The wind field agreement was actually better among the different systems than between any system and the buoys. However, the agreement among the analysis products was usually better for the zonal winds than for the meridional winds. For the time period and locations presented, the comparisons with the independent data show that no assimilation system is clearly superior to any of the others.

Rothstein, L.M., M.J. MCPHADEN, and J.A. Proehl. Wind forced wave-mean flow interactions in the equatorial waveguide. Part I: The Kelvin wave. *Journal of Physical Oceanography* 18(10):1435–1447 (1988).

A numerical model is designed to study the effects of the strong, near-surface shears associated with the equatorial current system on energy transmission of time-periodic equatorial waves into the deep ocean. The present paper is confined to long wavelength, low-frequency Kelvin waves forced by a longitudinally confined patch of zonal wind. Energy transmission into the deep ocean is investigated as a function of mean current shear amplitude and geometry and the forcing frequency. Solutions form well-defined beams of energy that radiate energy eastward and vertically toward the deep ocean in the absence of mean flow. However, the presence of critical surfaces associated with mean currents inhibits low-frequency energy from reaching the deep ocean. For a given zonal wavenumber, longitudinal propagation through mean currents will be less inhibited as the frequency increases (phase speed increases). When the mean current amplitude is large enough, the beam encounters multiple critical surfaces (i.e., critical surfaces for different wavenumber components of the beam) where significant exchanges of energy and momentum can take place with the mean currents via Reynolds stress transfers. Work against the mean vertical

shear is the dominant wave energy loss for the case of a mean South Equatorial Current-Equatorial Undercurrent system, illustrating the need for high vertical resolution in equatorial ocean models. The model also describes the possible induction of a mean zonal acceleration as well as a mean meridional circulation. Eliassen-Palm fluxes are used to diagnose these dynamics. The presence of critical surfaces result in mean field accelerations on the equator above the core of the Equatorial Undercurrent. Implications of these results with regard to observations in the equatorial waveguide are discussed.

JISAO PUBLICATIONS

Battisti, D.S. (1989): On the role of subtropical oceanic rossby waves during ENSO. *J. Phys. Oceanogr., 19*, 551-559.

Battisti, D.S., and A.C. Hirst (1989): Interannual variability in the tropical atmosphere/ocean system: influence of the basic state and ocean geometry. *J. Atmos. Sci., 46*, 1657-1712.

Giese, B.S. (1989): Equatorial oceanic response to forcing on time scales from days to months. NOAA Tech. Memo. ERL PMEL-87, 99 pp.

Harrison, D.E., and G.S. Giese (1989): Comment on "The response of the equatorial Pacific Ocean to a westerly wind burst in May 1986" by McPhaden *et al.* *J. Geophys. Res., 94*, 5024-5026.

Panetta, R.L., and I.M. Held (1989): Baroclinic eddy fluxes in a one-dimensional model of quasi-geostrophic turbulence. *J. Atmos. Sci., 45*, 3354-3365.

JIMAR PUBLICATIONS

Boehlert, G.W., and T. Sasaki (1988): Pelagic biogeography of the armorhead, *Pseudopentaceros wheeleri*, and recruitment to isolated seamounts in the North Pacific Ocean. *Fish. Bull. U.S., 86*, 453-456.

Caldwell, P., K. Wyrtki, and S. Nakahara (1989): TOGA Sea Level Center: Data from the Pacific. JIMAR Data Report No. 006, University of Hawaii.

Chiswell, S.M., and R. Lukas (1989): The low-frequency drift of Paroscientific pressure transducers. *J. Atmos. Oceanic Tech. 6*(3), 389-395.

Chiswell, S.M., and R. Lukas (1989): Rossby-gravity waves in the central equatorial Pacific during the NORPAX Hawaii-to-Tahiti Shuttle experiment. *J. Geophys. Res., 94*, 2091-2098.

Chu, P.-S. (1988): Extratropical forcing and the burst of equatorial westerlies in the western Pacific: A synoptic study. *J. Meteorol. Soc. Japan, 66*(4), 549-564.

Chu, P.-S. (1988): The use of meteorological information in forecasting Hawaiian drought. In: *Proceedings from the Drought Control and Water Management Workshop*, 1-2 November, Washington, D.C.

Chu, P.-S. (1989): On the origin and evolution of westerly wind bursts in the equatorial western Pacific during May 1982. Preprint Volume of the 18th Conference on Hurricanes and Tropical Meteorology, 16-10 May, San Diego, CA, 48-49.

Chu, P.-S., and R.W. Katz (1989): Spectral estimation from time series models with relevance to the southern oscillation. *J. Clim., 2*(1), 86-90.

Chu, P.-S., and R.W. Katz (1989): Spectrum of univariate time series models with application to the southern oscillation. Preprint Volume of the 4th International Meeting on Statistical Climatology, 27-31 March, Rotorua, New Zealand, 72-79.

Curtis, G. (1989): An unusual coastal hazard problem: Siting an ocean thermal energy conversion (OTEC) plant. In: *Natural and Man-Made Coastal Hazards*, S.F. Farreras and G. Pararas-Carayannis (eds.).

Curtis, G. (1989): Developing tsunami evacuation zones for Hawaii. In: *Proceedings of the Big Island Science Conference*, 10th Meeting, 21 April, Hilo, HI.

Firing, E. (1988): Mean zonal currents below 1500 m near the equator, 159°W. *J. Geophys. Res., 94*, 2023-2028.

Firing, E., R. Cabrera, and R. Lukas (1989): Currents in the central equatorial Pacific: An atlas of the Line Islands profiling project. JIMAR Report No. 89-0167, University of Hawaii.

Joyce, T., R. Lukas, and E. Firing (1989): On the hydrostatic balance and equatorial geostrophy. *Deep Sea Res., 35*, 1255-1257.

Lamadrid-Rose, Y., and G.W. Boehlert (1988): Effects of cold shock on egg, larval and juvenile stages of tropical fishes: Potential impacts of ocean thermal energy conversion. *Mar. Env. Res., 25*, 175-193.

Lukas, R. (1988): Freshwater input to the western equatorial Pacific Ocean and air-sea interaction. In: *Proceedings of the Symposium on Western Tropical Pacific Air-Sea Interactions*, 5-17 November, Beijing, China.

Lukas, R. (1989): The impact of clouds and fresh water flux on the dynamics and thermodynamics of the tropical ocean. Preprint Volume of the Symposium on the Role of Clouds in Atmospheric Chemistry and Global Climate, 30 January - 2 February, Anaheim, CA, 35-38.

Mader, C., and G.T. Mitchum (1988): Tsunami modeling using personal computers. In: *Proceedings of the Pacific Congress on Marine Science and Technology*, 16-20 May, Honolulu, HI.

Mader, C. (1989): Numerical modeling of the effect of particle size of explosives on shock initiation properties. In: *Proceedings of the 4th International Congress of Pyrotechniques*, La Grande-Motte, France.

Mader, C., and J.D. Kershner (1989): The heterogeneous explosive reaction zone. In: *Proceedings of the 9th International Symposium on Detonation.*

Morrissey, M., and M.A. Lander (1988): Climatology of west wind bursts in the equatorial western Pacific and their relationship to El Niño. In: *Proceedings of the Climate Diagnostics Workshop*, 31 October-5 November, Cambridge, MA, 127-132.

Roach, D., G.T. Mitchum, and K. Wyrtki (1989): Length scales of interannual sea level variations along the Pacific margin. *J. Phys. Oceanogr., 19*(1), 122-128.

Rui, H., and B. Wang (1989): Evolution and structure of tropical intraseasonal convection anomalies. In: *Proceedings of the 18th Conference on Hurricanes and Tropical Meteorology*, 16-19 May, San Diego, CA.

Stommel, H., and D. Moore (1989): *An Introduction to the Coriolis Force*. Columbia University Press, New York, 297 pp.

Wang, B. (1988): Comments on "An air-sea interaction model of intraseasonal oscillation in the tropics." *J. Atmos. Sci., 45*(22), 3521-3525.

Wyrtki, K., and G.T. Mitchum (1988): The global sea level observing system. In: *Proceedings of the Joint Oceanographic Assembly*, 23-31 August, Acapulco, Mexico.

CIMRS PUBLICATIONS

Embley, R.W., S.R. Hammond, and K. Murphy (1988): The caldera of Axial Volcano – remote sensing and submersible studies of a hydrothermally active submarine volcano. In: *Global Venting, Midwater, and Benthic Ecological Processes* (M.P. De Luca and I. Babb, eds.), National Undersea Research Program Report 88-4, 61-70.

Fox, C.G., and M. van Heeswijk (1988): Sea Beam backscatter analysis applied to the classification of deep-sea volcanic terrains. In: *Global Venting, Midwater, and Benthic Ecological Processes* (M.P. De Luca and I. Babb, eds.), National Undersea Research Program Report 88-4, 71-79.

GLOSSARY OF ACRONYMS

ACC:	Alaska Coastal Current
ADCP:	Acoustic Doppler Current Profiler
ADIOS:	Asian Dust Input to the Oceanic System
AID:	Agency for International Development
AL:	Aeronomy Laboratory (ERL)
AOML:	Atlantic Oceanographic and Meteorological Laboratory (ERL)
APEX:	Arctic Polynya Experiment
ARGOS:	French satellite used to telemeter data to shore stations (not an acronym)
ARL:	Air Resources Laboratory (ERL)
ASG:	Administrative Support Group
ASHES:	Axial Seamount Hydrothermal Emissions Study
ATLAS:	Automated Temperature Line Acquisition System
AVHRR:	Advanced Very-High-Resolution Radiometer
BPR:	Bottom Pressure Recorder
BT:	Bathythermograph
CEAREX:	Coordinated Eastern Arctic Experiment
CMDL:	Climate Monitoring and Diagnostics Laboratory
CIMRS:	Cooperative Institute for Marine Resources Studies
CIRES:	Cooperative Institute for Research in Environmental Sciences
CITE-3:	Chemical Instrumentation and Test Evaluation (NASA)
COADS:	Comprehensive Ocean-Atmosphere Data Set
COARE:	Coupled Ocean-Atmosphere Response Experiment
CRF:	Cloud Radiation Feedback
CSG:	Computer Support Group
CTD:	Conductivity, Temperature, Depth
DOD:	Department of Defense
DOE:	Department of Energy
EDD:	Engineering Development Division
ENSO:	El Niño-Southern Oscillation
EOF:	Empirical Orthogonal Function
EPOCS:	Equatorial Pacific Ocean Climate Studies
ERL:	Environmental Research Laboratories (NOAA)
FAST:	Flow Actuated Sediment Trap
FGGE:	First GARP Global Experiment
FNOC:	Fleet Numerical Oceanography Center
FOCAL:	French Program Ocean-Climat Atlantique Equatorial
FOCI:	Fisheries-Oceanography Coordinated Investigations
FOCUS:	Fisheries Oceanography Cooperative Users System
FOX:	Fishery-Oceanography Experiment
FREEZE:	Name of arctic ice formation experiment (not an acronym)
FSL:	Forecast Systems Laboratory (ERL)
GARP:	Global Atmospheric Research Program
GFDL:	Geophysical Fluid Dynamics Laboratory (ERL)

GLERL:	Great Lakes Environmental Research Laboratory (ERL)
GMC:	General Circulation Model
GMCC:	Geophysical Monitoring for Climatic Change (ARL)
GOES:	Geostationary Operational Environmental Satellite
HMSC:	Hatfield Marine Science Center
HOT:	Hawaiian Ocean Time series
IAMAP/IAPSO:	International Assosciation of Meteorology and Atmospheric Physics/International Association for the Physical Sciences of the Ocean
IGOSS:	International Global Ocean Services System
IGSP:	International Greenland Sea Project
IOC:	International Oceanographic Commission
IRIS:	International Recruitment Investigations in the Subarctic
ITCZ:	Intertropical Convergence Zone
JIC:	Navy/NOAA Joint Ice Center
JIMAR:	Joint Institute for Marine and Atmospheric Research
JISAO:	Joint Institute for the Study of Atmosphere and Ocean
L-RERP:	Long-Range Effects Research Program
MARD:	Marine Assessment Research Division
MIZ:	Marginal Ice Zone
MIZEX:	Marginal Ice Zone Experiment
MMS:	Minerals Management Service, U.S. Dept. of Interior
MRRD:	Marine Resources Research Division
MSRD:	Marine Services Research Division
NASA:	National Aeronautics and Space Administration
NCAR:	National Center for Atmospheric Research
NESDIS:	National Environmental Satellite, Data, and Information Service (NOAA)
NGM:	Nested Grid Model
NIC:	NOAA Information Center
NMC:	National Meteorological Center (NOAA)
NMFS:	National Marine Fisheries Service (NOAA)
NOAA:	National Oceanic and Atmospheric Administration
NORPAX:	North Pacific Experiment
NOS:	National Ocean Service (NOAA)
NSF:	National Science Foundation
NSSL:	National Severe Storms Laboratory (ERL)
NWAFC:	Northwest and Alaska Fisheries Center
NWS:	National Weather Service (NOAA)
OAR:	Oceanic and Atmospheric Research
OCEAN STORMS:	A JISAO field experiment for the assessment of weather fronts (not an acronym)
OCRD:	Ocean Climate Research Division
OCS:	Outer Continental Shelf
OLR:	Outgoing Longwave Radiation
PACTOP:	Pacific Tsunami Observation Program
PEGASUS:	Current velocity profiling instrument (not an acronym)
PENTAFLUX:	Fifth Flux Experiment
PEQUOD:	Pacific Equatorial Ocean Dynamics
PMEL:	Pacific Marine Environmental Laboratory (ERL)
POSEIDON:	French component of joint U.S./French TOPEX/POSEIDON sea-surface topography satellite mission (not an acronym)

PSI:	Pacific Sulfur/Stratus Investigation
Ri:	Richardson Number, a dimensionless number related to stability of stratified flow
RITS:	Radiatively Important Trace Species
RJE:	Remote Job Entry
SCOR:	Scientific Committee on Oceanic Research
SEABEAM:	A shipboard multi-transducer swath echo sounding system
SEL:	Space Environment Laboratory (ERL)
SLAR:	Side-Looking Airborne Radar
SLEUTH:	System for Locating Eruptive Underwater Turbidity and Hydrography
SLP:	Sea Level Pressure
S^3T:	Sequentially Sampling Sediment Trap
SST:	Sea Surface Temperature
STACS:	Subtropical Atlantic Climate Studies
TAG:	Trans Atlantic Geotraverse
TAO:	Thermal Array for the Ocean; Tropical Atmosphere/Ocean
THRUST:	Tsunami Hazard Reduction Using System Technology
TOGA:	Tropical Oceans and Global Atmosphere
TOPEX:	Topographic Experiment (NASA)
TOPS:	Total Ocean Profiling System
USGS:	United States Geological Survey
VENTS:	Name of hydrothermal venting research program (not an acronym)
WEPOCS:	Western Equatorial Pacific Ocean Circulation Study
WMO:	World Meteorological Organization
WOCE:	World Ocean Circulation Experiments
WPL:	Wave Propagation Laboratory (ERL)
XBT:	Expendable Bathythermograph